Quantitative Analysis of Werner Helicase Activity Using the Single-Molecule Fluorescence Detection System MF10S

Kazunobu FUTAMI, Hideyuki GOTO, Akira SHIMAMOTO, Takahide WATANABE, and Yasuhiro FURUICHI*

GeneCare (previously AGENE) Research Institute; 200 Kajiwara, Kamakura, Kanagawa 247–0063, Japan.
Received August 9, 2004; accepted September 19, 2004

We developed a system that uses the single-molecule fluorescence detection system MF10S to assess quantitatively the activity of WRN helicase, the product of the causative gene of Werner syndrome that includes premature ageing. Double-strand DNA substrates labeled with the fluorescence dye TAMRA at the 5′ end and with a quencher at the 3′ end of the counter strand were incubated with a single trapper oligonucleotide and Werner helicase, and the resultant single DNA fragments labeled with TAMRA produced by the unwinding of WRN helicase were detected using the MF10S. The results using this system and those using polyacrylamide gel electrophoresis were well correlated. The MF10S system provides a quantitative analysis that is much faster, simpler, and more economical than systems using polyacrylamide gel electrophoresis and radioisotopes, and could be used as a quantitative analysis system for Werner helicase and other DNA helicase activities.

Key words helicase assay; screening system; anti-cancer drug

Inhibitors of DNA helicases have potential applications to screen anti-virus and anti-tumor drugs. The screening of compounds to inhibit helicases of hepatitis C virus (NS3), herpes simplex virus (UL5), and papillomavirus has been reported.[1—4] WRN helicase, the product of the causative gene of Werner syndrome, unwinds double-strand DNA.[5,6] Short interference RNAs (siRNAs) with WRN gene sequences inhibit the expression of WRN helicase in HeLa cells resulting in genomic instability (Futami *et al.*, unpublished results). Cells lacking WRN helicase have increased sensitivity to cytotoxicity by camptothecin.[7] Thus, the development of a system to quantitatively assay DNA helicases, including WRN helicase, is necessary not only for research, but also for highly sensitive screening of anti-virus and anti-cancer drugs without using radioisotopes. We report here a system enabling the DNA-unwinding activity of Werner helicase to be quantitatively assayed and monitored using the single-molecule fluorescence detection system MF10S.

MATERIALS AND METHODS

Sequences of the double-strand DNA substrate were: 1) donor strand oligonucleotide, 5′-TAMRA (6-carboxytetramethylrhodamine)-TAGTACCGCCACCCTCAGAACCTTTTTTTTTTTTTTT; and 2) acceptor strand, 5′-TAGTACCGCCACCCTCAGAACC-BHQ (Black Hole Quencher)-2; 3) A-trapper, 5′-TAGTACCGCCACCCTCAGAACC; 4) B-trapper, 5′-GGTTCTGAGG-GTGGCGGTACTA. Actinomycin D, adenosine 5′-*O*-(3-thiotriphosphate) (ATP-γ-S) and SYBR Gold (SYBR® Gold) were purchased from Sigma (St. Louis), Roche Diagnostic (Tokyo) and Molecular Probes (Oregon), respectively. TAMRA- and BHQ-2-labeled oligonucleotides were obtained from Hokkaido System Science Co., Ltd. (Sapporo). The substrate oligonucleotide DNAs were prepared by heating single oligonucleotides at 90 °C for 5 min and then by cooling to room temperature. TAMRA is a stable dye, and BHQ-2 is a highly efficient quencher that strongly prevents fluorescence of TAMRA without emitting its own fluorescence leading to a low background. This TAMRA/BHQ-2 system has an advantage over a system using a quencher that is based on a distance-dependent fluorescence resonance energy transfer.[8—10]

Preparation of WRN Helicase WRN helicase was expressed using the baculovirus vector/Sf9 system, and was purified as previously reported.[11] Briefly, infected cells were collected and resuspended in ice-cold PBS and the recombinant proteins were purified by 6×His affinity chromatography.

Helicase Assay The reaction conditions for WRN helicase activity were optimized with 50 μl of reaction mixture containing 50 mM Tris–HCl (pH 7.5), 2 mM 2-Mercapto ethanol, 5 mM $MgCl_2$, 1 mM ATP, 20 μg/ml bovine serum albumin, 90 mM NaCl, 5 nM WRN helicase, 2 nM DNA substrate, and the trapper single strand DNA at various concentrations in glass bottom 96-well plates (Whatman, Clifton, NJ, U.S.A.). The reaction was done at 37 °C for the indicated period shown as the "reaction time" in each figure, and then was stopped by adding 10 μl of 5× stopping dye solution containing 0.1% xylene cyanol (Nacalai Tesque, Kyoto), 100 mM Tris–HCl, and 50% glycerol. The reaction mixtures in 96-well plates were read using an Olympus MF10S (543 nm, laser power; 300 μW, 0.5 S) three times for each well, and an aliquot of each reaction mixture was analyzed using 15% polyacrylamide gel electrophoresis (PAGE) with an electrophoresis buffer (pH 8.5) consisting of 0.09 M Tris–borate and 2 mM ethylenediaminetetraacetic acid (EDTA). After electrophoresis (20 min, 200 V/4 cm), the gel was visualized by laser scanning in an fluorescent image analyzer FMBIO® II Multi-View and FMBIO Analysis version 6.0 software (Hitachi Software Engineering, Yokohama).

Fluorescence Detection System MF10S We used a MF10S (Olympus) single-molecule fluorescence detection system for quantitative analysis of unwound TAMRA-labeled DNA strands. This system permits the detection of fluorescent signals coming from a small volume (10^{-15} l) of reaction mixture by the optics of a confocal microscope. Samples at several nanomolar concentrations contain a few molecules in the volume, so signals directly reflect the intensity and the number of fluorescent molecules. The number of fluorescent signals was expressed by the "countrate" that indicates the

* To whom correspondence should be addressed. e-mail: furuichi@genecare.co.jp

number of photons in each second detected in an area being measured.[12]

RESULTS AND DISCUSSION

We chose TAMRA as a reporter because it is easy to label the substrate oligonucleotides and is not expensive. We then compared the sensitivity to detect TAMRA-labeled DNAs between two detection systems, the MF10S and a Wallac multilabel counter (Perkin-Elmer, Tokyo) which is often used for high-throughput screening (HTS) (Fig. 1). The sensitivity with the MF10S system was found to be about 100-fold higher than that of the Wallac system, and moreover, the background associated with MF10S was low, giving rise to the reproducible results. As a result, the combination of TAMRA and MF10S could reduce the amounts of both substrate and enzyme, rendering the system almost equivalent to the radioisotopic system. Based on these results, we applied the MF10S system for helicase assay. An assay system for WRN helicase that uses the MF10S single-molecule fluorescence detection system was assessed under various reaction conditions and the results were compared with the results obtained from PAGE analysis simultaneously done using the same reaction products.

Effect of Trappers WRN helicase unwinds double strand DNA.[6,11,13] The unwinding reaction of double-strand DNA by WRN helicase requires trappers *in vitro* to stabilize the resultant single strand DNA by preventing reannealing.[14] Figure 2 shows the outline of the reaction. The efficiency of two types of trapper oligonucleotides, A-trapper and B-trapper, for binding the unwound DNA strand was compared (Fig. 2A). A-trapper and B-trapper form duplexes with BHQ-2 labeled and TAMRA-labeled strands, respectively. The partially double-stranded DNA substrates consisting of TAMRA-labeled and BHQ-2-labeled strands were mixed with either A-trapper or B-trapper, and the mixture was incubated with Werner helicase. The trappers inhibited re-formation of the duplex between the original substrate DNA strands, making the detection of reaction products more efficient. The fluorescence of TAMRA near BHQ in duplex oligonucleotides was suppressed to very low levels, but the fluorescence of TAMRA in a single oligonucleotide apart from BHQ was strong. Figure 2B shows the results of the analysis using the Olympus MF10S. A-trapper was more efficient than B-trapper, which was confirmed by the assay that used PAGE (Fig. 2C). Therefore, we used A-trapper in the following experiments.

Dose Dependency of A-Trapper Figure 3A shows the dose-dependency of A-trapper in the assay using the MF10S. The unwinding reaction nearly reached a plateau at 50 nM of A-trapper. A similar result was obtained by the independent assay system using PAGE. The good correlation between the results by MF10S and PAGE guarantees that the system using MF10S could be used for quantitative assay of WRN

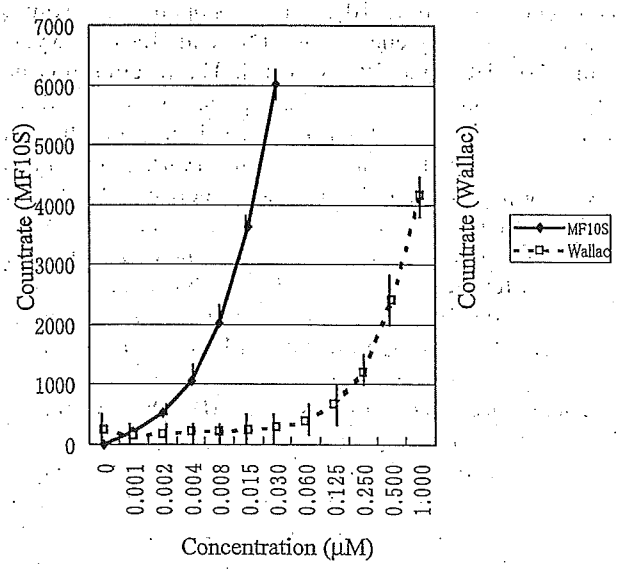

Fig. 1. Comparison of Sensitivity between MF10S and Wallac Systems

The countrate of TAMRA-labeled oligonucleotide was determined either by the MF10S or Wallac system. Vertical and horizontal axes indicate countrate and concentration (μM) of TAMRA-labeled oligonucleotide, respectively. Each point represents a mean of 5 samples and vertical bars indicate standard deviation.

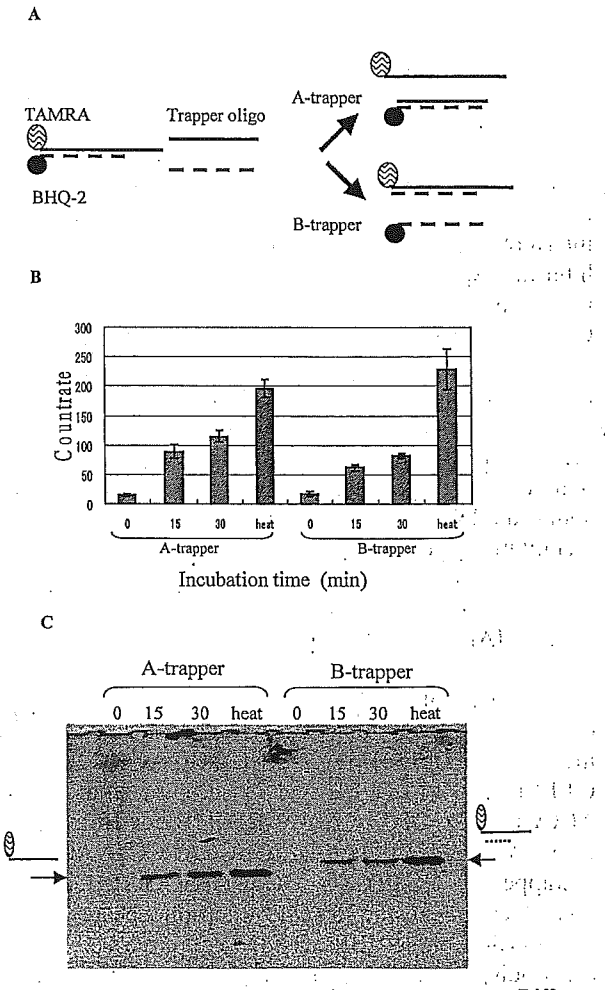

Fig. 2. Assay of Werner Helicase Activity by Using Two Different Oligonucleotides as Trapper Molecules; One Is Complementary to TAMRA-Labeled Oligonucleotide and the Other Is Complementary to BHQ-2-Labeled Oligonucleotide

(A) Two kinds of reaction products forming a duplex with A-trapper or B-trapper are shown. (B) Fluorescence values and the countrate are shown in a Werner helicase reaction with A-trapper or B-trapper by measuring with the MF10S. Each column indicates the mean of three measurements and vertical bars indicate standard deviation. (C) TAMRA fluorescence image in polyacrylamide gel is shown for the same samples of the reaction of B. A TAMRA fluorescence image obtained using an FMBIO II image analyzer. Excitation was 532 nm laser light. The arrows show the position of the TAMRA- labeled oligonucleotide forming a duplex with A-trapper or B-trapper.

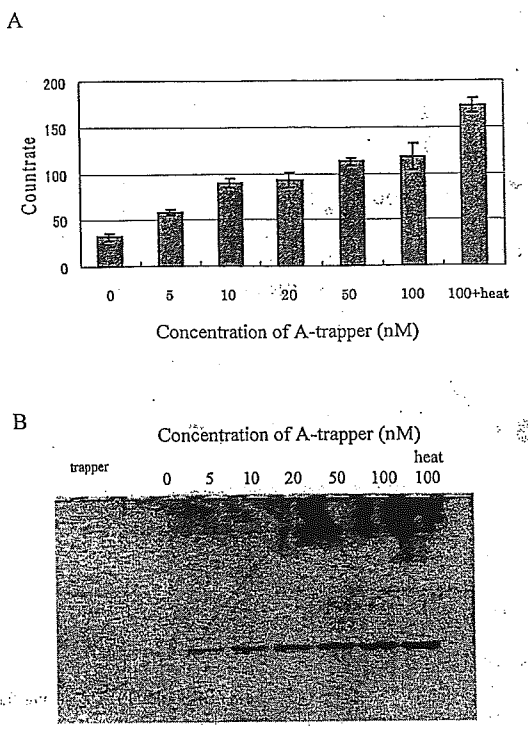

Fig. 3. Dose-Dependency of A-Trapper in a Werner Helicase Reaction, Which Has the Complementary Oligonucleotide Sequence to the BHQ-2-Labeled Sequence

(A) The reaction products are expressed as the countrate using the MF10S. See also the legend of Fig. 2B. (B) The same reaction products are represented as the fluorescence image of TAMRA after the PAGE of each sample.

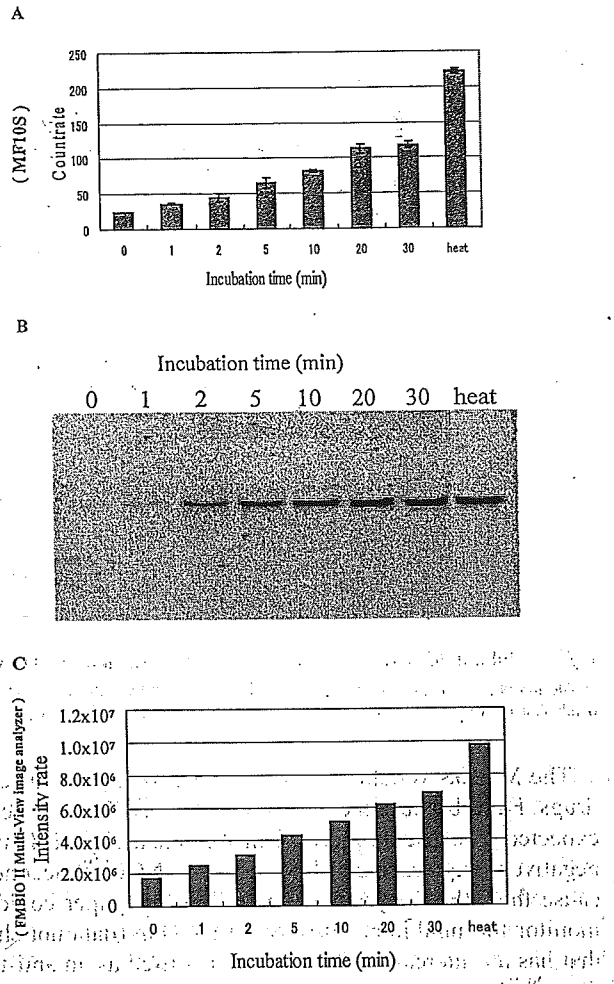

Fig. 4. Time Course of Werner Helicase Reaction Measured by the MF10S (A) and PAGE (B)

See also the legend of Fig. 2B (C). The intensity of fluorescence image of each band was calculated using Image Analysis Software (Hitachi Software Co., Ltd.).

helicase and other DNA helicases instead of PAGE using radioisotopes. The exonuclease consisting of an integral part of Werner helicase[6,15] does not seem to affect the assay system under the conditions tested in this study.

Time Course Figure 4A and 4B show the time course of the reaction using the Olympus MF10S and PAGE, respectively. Figure 4C shows the quantitative intensity of the fluorescence image after the PAGE, which was calculated by image-analysis software. In both assay systems, the reaction nearly reached a plateau after 20 min. Thus, this system can monitor in real-time a helicase-catalyzed reaction process by using the increase in fluorescence.

Effects of Inhibitors The effects of three kinds of inhibitors on Werner helicase activity were investigated to test if the MF10S system can detect inhibitors of WRN helicase. Actinomycin D, an antineoplastic antibiotic that forms a stable complex with DNA, inhibited the activity of Werner helicase at 10 μg/ml (8 μM) or below, reaching a plateau at 20 μg/ml (16 μM) or more, and had a maximal inhibitory effect of about 30% (Fig. 5A, D). ATPγS, which inhibits ATP-dependent enzymes by competing with ATP, showed a more than 60% inhibitory effect at 20 μg/ml (36.6 μM) (Fig. 5B, E). SYBR Gold, a reagent that has a high affinity for DNA and RNA, showed about 70% inhibition at a concentration of 10^{-3} dilution of the original solution when analyzed by a standard 300 nm UV transilluminator. SYBR Gold has strong fluorescence by itself, and it interfered with the assay system (Fig. 5C): The fluorescence of SYBER Gold was visible as strong bands at the top of the PAGE gel (Fig. 5F). These results indicate that the MF10S system can be used as a screening system for compounds that show anti-WRN helicase activity.

Thus far helicase activity has been identified by the reaction products of radioisotope-labeled substrates using PAGE. High-throughput screening systems based on fluorescence resonance energy transfer (FRET) also have been developed.[8,9,16–18] The FRET system is proven to be useful to monitor the reactions catalyzed by helicase, because the results by two systems using radioisotopes and fluorescence coincided very well.[15] Comparing these systems, the MF10S system has the following advantages: 1) the cost of the assay system is cheaper and a high signal-to-noise ratio was achieved by using the strong, dark quencher BHQ. 2) simultaneous monitoring of enzymatic analysis using the same reaction products by MF10S and PAGE is possible, enabling the compounds to be assessed by indigenous fluorescence, as seen with SYBR Gold (Fig. 5C, F); 3) MF10S is more sensitive than FRET because the optics of a confocal microscope are used; 4) problems due to air bubbles as seen with the FRET system are avoided because the MF10S system allows fluorescent signals to come from a small volume element (10^{-15} l); and 5) the time required for analysis is much shorter compared with the PAGE-radioisotope system that is often accompanied by a degradation of compounds.

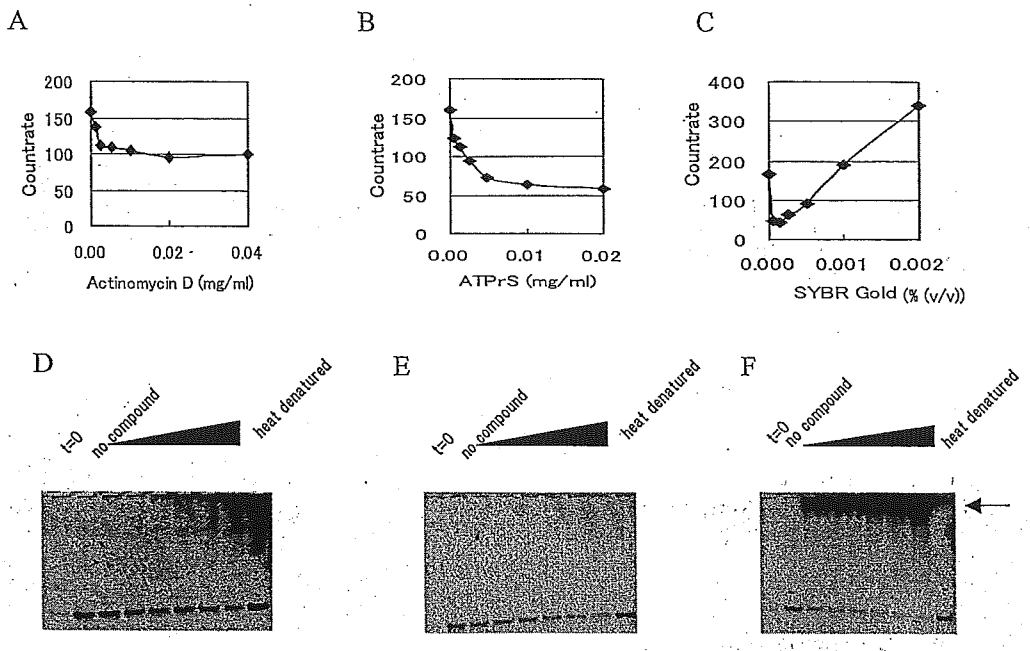

Fig. 5. Inhibition of Werner Helicase Activity by Actinomycin D (A), ATPγS (B) and SYBR Gold (C)

The inhibition was measured using the MF10S. The same samples were also analyzed by PAGE: actinomycin D (D), ATPγS (E) and SYBR Gold (F). The strong fluorescent band near the wells in F is due to the fluorescence of SYBR Gold itself which is also reflected in the increase in the countrate at higher doses in C.

The MF10S system has the potential to screen anti-cancer drugs. First, because the down-regulation of WRN helicase is expected to cause an increase in the sensitivity of dominant negatively expressed cell lines against 4NQO.[19] Second, because the MF10S system described in this paper could also monitor the inhibitory effect of adriamycin (data not shown) that has an intercalating activity and is used as an anti-tumor drug.[20,21]

Acknowledgements We thank Mr. Kazuhito Gohda, Genome Medical Business Division, Olympus Optical Co., Ltd. for his help in the assay using the MF10S single-molecule fluorescence detection system, and Dr. Masanobu Sugimoto of GeneCare Research Institute Co., Ltd. for his invaluable discussion and help to prepare this manuscript.

REFERENCES

1) Borowski P., Niebuhr A., Schmitz H., Hosmane R. S., Bretner M., Siwecka M. A., Kulikowski T., *Acta Biochimica Polonica*, **49**, 597—614 (2002).
2) Crute J. J., Grygon C. A., Hargrave K. D., Simoneau B., Faucher A.-M., Bolger G., Kibler P., Liuzzi M., Cordingley M. G., *Nature Medicine*, **8**, 386—391 (2002).
3) Kleymann G., Fischer R., Betz U. A. K., Hendrix M., Bender W., Schnetder U., Handke G., Eckenberg P., Hewlett G., Pevzner V., Baumeister J., Weber O., Henninger K., Keldenich J., Jensen A., Kolb J., Bach U., Popp A., Maben J., Frappa I., Haebich D., Lockhoff O., Rubsamen-Waigmann H., *Nature Medicine*, **8**, 392—398 (2002).
4) Faucher A. M., White P. W., Brochu C., Grand-Maitre C., Rancourt J., Fazal G., *J. Med. Chem.*, **47**, 18—21 (2004).
5) Yu C. E., Oshima J., Fu Y. H., Wijsman E. M., Hisama F., Alisch R., Matthews S., Nakura J., Miki T., Ouais S., Martin G. M., Mulligan J., Schellenberg G. D., *Science*, **272**, 258—262 (1996).
6) Shimamoto A., Sugimoto M., Furuichi Y., *Int. J. Clin. Oncol.*, **9**, 288—298 (2004).
7) Okada M., Goto M., Furuichi Y., Sugimoto M., *Biol. Pharm. Bull.*, **21**, 235—239 (1998).
8) Stryer L., Haugland R. P., *Proc. Natl. Acad. Sci. U.S.A.*, **58**, 719—726 (1967).
9) Parkhurst K. M., Parkhurst L. J., *Biochemistry*, **34**, 293—300 (1995).
10) Parkhurst K. M., Parkhurst L. J., *Biochemistry*, **34**, 285—292 (1995).
11) Suzuki N., Shimamoto A., Imamura O., Kuromitsu J., Kitao S., Goto M., Furuichi Y., *Nucleic Acids Res.*, **25**, 2973—2978 (1997).
12) Kato N., Okamoto N., Kobayashi S., Otsuka C., Nagano T., *Idenshi-igaku*, **6**, 271—277 (2002) (in Japanese).
13) Lohman T. M., Bjornson K. P., *Ann. Rev. Biochem.*, **65**, 169—214 (1996).
14) Houston P., Kodadek T., *Proc. Natl. Acad. Sci. U.S.A.*, **91**, 5471—5474 (1994).
15) Choudhary S., Sommers J. A., Brosh R. M., Jr., *J. Biol. Chem.*, **279**, 34603—34613 (2004).
16) Haupts U., Rudiger M., Ashman S., Turconi S., Bingham R., Wharton C., Hutchinson J., Carey C., Moore K. J., Pope A. J., *J. Biomolecular Screen.*, **8**, 19—33 (2003).
17) Jager S., Brand L., Eggeling C., *Curr. Pharm. Biotechnol.*, **4**, 463—476 (2003).
18) Earnshaw D. L., Moore K. J., Greenwood C. J., Djaballah H., Jurewicz A. J., Murray K. J., Pope A. J., *J. Biomolecular Screen.*, **4**, 329—247 (1999).
19) Bai Y., Murnane J. P., *Hum. Genet.*, **113**, 337—347 (2003).
20) Kanter P. M., Schwartz H. S., *Leuk Res.*, **3**, 277—283 (1979).
21) Cullinane C., Cutts S., Panousis M. C., Phillips D. R., *Nucleic Acids Res.*, **28**, 1019—1012 (2000).

Gene Transfer to Corneal Epithelium and Keratocytes Mediated by Ultrasound with Microbubbles

Shozo Sonoda,[1] Katsuro Tachibana,[2] Eisuke Uchino,[1] Akiko Okubo,[1] Matsuo Yamamoto,[3] Kenji Sakoda,[4] Toshio Hisatomi,[5] Koh-Hei Sonoda,[5] Yoichi Negishi,[6] Yuichi Izumi,[4] Sonshin Takao,[7] and Taiji Sakamoto[1]

Purpose. The cornea is an ideal organ for evaluating gene transfer because it can be treated noninvasively and monitored easily. The present study was performed to investigate the practical efficacy and safety of ultrasound (US) plus microbubble (MB)–mediated gene transfer to cornea.

Methods. Cultured rabbit corneal epithelial (RC-1) cells were incubated in 24-well dishes with plasmid DNA having a green fluorescent protein (GFP) gene under a cytomegalovirus promoter. The cells were exposed to US under different intensities (1 MHz; power, 0.5~2 W/cm^2; duration, 15–120 seconds; duty cycle, 20%–100%). The effect of simultaneous stimulation with MBs was also examined. Gene transfer was quantified by counting the number of GFP-positive cells under microscopy. Furthermore, in vivo gene transfer was examined by GFP plasmid injection into rabbit cornea and US exposure with MBs.

Results. In the in vitro study, DNA exposure alone could not transfer gene into cultured RC-1 cells; US enhanced gene transfer slightly. Coexposure with MBs significantly increased gene transfer efficiency. In the in vivo study, DNA injection alone could transfer the gene to a limited degree, but plasmid injection plus US with MBs strongly increased gene transfer efficiency without apparent tissue damage, and gene transfer was achieved two dimensionally.

Conclusions. US with MBs greatly increases gene transfer to in vivo and in vitro corneal cells. This noninvasive gene transfer method may be a useful tool for clinical gene therapy. (*Invest Ophthalmol Vis Sci.* 2006;47:558–564) DOI:10.1167/iovs.05-0889

A modality to efficiently deliver genes to living tissue is essential for gene therapy and genetic research. The basic technology of gene delivery can be divided into two categories, a virus vector–mediated method and a non-virus vector–mediated method.[1–3] The virus vector–mediated method can transfer the gene of interest with high efficiency, but concern about safety issues prevents clinical application for common diseases.[3–5] The non-virus vector–mediated method is comparatively safe, but gene transfer efficiency does not reach a satisfactory level.[6–9] Among these methods, the mechanical enhancing method is unique because it is free from a biochemical agent that has not been proven to be safe for humans; thus, clinical application might be more easily accepted. Electroporation can be used for this purpose but often results in severe cell damage.[10,11] In contrast, it recently became apparent that ultrasound (US) can enhance gene transfer to mammalian cells in vitro and in vivo without cell damage,[12–16] and US-mediated gene therapy has been reported in vessels and muscles of animal studies.[17,18] US is now widely used for clinical examinations and therapies, and its safety has been reliably established.

The cornea plays an important role in maintaining vision. Vision can be seriously impaired as a result of corneal cloudiness caused by insufficient wound healing or by the metabolic processes of cornea. Although corneal surgery is widely performed and may be performed even more often as more refractive surgery is performed, the cellular and molecular events that control wound healing within the corneal stroma are not well understood.[19,20] The cornea is an external tissue suitable for gene therapy because of its easy accessibility by surgical maneuvers, including US. In addition, gene transfer can be easily monitored by noninvasive methods such as microscopic observation.[21]

Microbubbles (MBs), which are gas bubbles measuring approximately 3 μm in diameter, have been developed mainly as contrast agents to improve ultrasonographic images. They have shown promise in gene therapy for several reasons. MBs act as cavitation nuclei, effectively focusing ultrasound energy, and they can potentiate bioeffects. Evidence indicates that the ultrasound energy needed can be greatly reduced; therefore, the lower power used in diagnostic imaging systems may be sufficient to produce therapeutic effects.[22–24]

Simultaneous use of US and MBs has been found to increase gene transfer efficiency.[25–32] However, to our knowledge, few reports have been published of detailed analyses of US-mediated gene transfer with MBs. In this study, we performed a detailed analysis of gene transfer mediated by US with MBs using cornea, and we show two-dimensional gene transfer achieved by this method.

Methods

In Vitro Study

Cell Culture. Rabbit corneal epithelial (RC-1) cells (JCRB0246) were obtained from Human Science Research Resource Bank (Tokyo, Japan) and incubated in modified Eagles medium (MEM; Sigma-Aldrich, St. Louis, MO) with 10% fetal bovine serum (FBS; Invitrogen-Gibco, Grand Island, NY) and streptomycin/penicillin (Wako, Osaka, Japan). All cells used in the studies were from passages 4 to 6.

From the Departments of [1]Ophthalmology and [4]Periodontology and the [7]Research Center for Life Science Resources, Kagoshima University, Kagoshima, Japan; the [2]Department of Anatomy, Fukuoka University School of Medicine, Fukuoka, Japan; the [3]Department of Periodontology, Showa University School of Dentistry, Tokyo, Japan; the [5]Department of Ophthalmology, Graduate School of Medical Sciences, Kyushu University, Fukuoka, Japan; and the [6]School of Pharmacy, Tokyo University of Pharmacy and Life Sciences, Tokyo, Japan.

Supported by Grants-in-Aid for Scientific Research (17390469 and 14370560) and Grant-in-Aid for Young Scientists (16791056) from the Ministry of Education, Science and Culture of the Japanese Government.

Submitted for publication July 11, 2005; revised September 9, 2005; accepted December 22, 2005.

Disclosure: **S. Sonoda**, None; **K. Tachibana**, None; **E. Uchino**, None; **A. Okubo**, None; **M. Yamamoto**, None; **K. Sakoda**, None; **T. Hisatomi**, None; **K.-H. Sonoda**, None; **Y. Negishi**, None; **Y. Izumi**, None; **S. Takao**, None; **T. Sakamoto**, None

The publication costs of this article were defrayed in part by page charge payment. This article must therefore be marked "*advertisement*" in accordance with 18 U.S.C. §1734 solely to indicate this fact.

Corresponding author: Taiji Sakamoto, Department of Ophthalmology, Kagoshima University Faculty of Medicine, 8-35-1 Sakuragaoka, Kagoshima, Japan 890-8520; tsakamot@m3.kufm.kagoshima-u.ac.jp.

Investigative Ophthalmology & Visual Science, February 2006, Vol. 47, No. 2

Plasmids. An expression vector for the green fluorescent protein (GFP) gene, *pEGFP-N2*, a mammalian expression vector containing a cytomegalovirus immediate-early enhancer/promoter, was obtained from Clontech Co., Ltd. (Palo Alto, CA). Plasmids grown in *Escherichia coli* host strain XLI-blue were purified (Plasmid Kit; Qiagen, Valencia, CA) and suspended in TE buffer (pH 8.0) at a concentration of 1.0 μg/μL. Plasmids were then suspended in phosphate-buffered saline (PBS; Invitrogen-Gibco), and the pH was adjusted to 7.35.

Ultrasound Exposure. RC-1 cells were collected with trypsin (Sigma-Aldrich), passed through a cell strainer (Becton Dickinson, Franklin Lakes, NJ), and put into a 48-well collagen type 1-coated glass bottom chamber (Asahi Technoglass, Chiba, Japan) filled with 400 μL MEM with 10% FBS, 4×10^4cells/well. A plasmid solution 0.5 μL was added to the medium. Immediately thereafter, US was exposed to the medium using a 6-mm probe generated by an US machine (Sonitron 2000; Richmar, Inola, OK). During exposure, the medium-containing cells were gently stirred by a magnetic stirrer (300 rpm). To induce MBs, perflutren protein type A microsphere (Optison; Amersham Health, Princeton, NJ)—a well-established, second-generation US medical diagnostic product with robust capability—was used. It is an albumin-shelled US contrast agent composed of approximately 5 to 8×10^8 MBs per milliliter measuring between 2 and 4.5 μm in diameter and filled with octaperfluoropropane. The indicated percentage was added to the plasmid solution (0.5, 0.25, or 0.1 μL), gently mixed, and left for 60 seconds. Immediately thereafter, the mixed solution was added to the dish and exposed to US as described.

Gene Transfer Efficiency. After gene transfer treatment, including plasmid alone or plasmid plus US exposure, the cells were incubated in a medium containing 10% FBS for 48 hours and then were observed by phase-contrast microscopy with or without a 515-nm filter (Olympus, Tokyo, Japan). A randomly selected field (4 fields/well with 100 × magnification) was photographed. The photographs were monitored by a NIH image analyzer, and the ratio of GFP-positive cells to all cells in each field was evaluated by masked observers. To determine the duration of GFP expression, GFP expression was evaluated on days 4, 8, 14, and 30.

Cell Survival and Cell Damage. Survival of cells was evaluated by counting living cells. Briefly, after 48 hours of incubation, the dishes were washed twice with PBS, four microscopic fields per well were photographed, and the living cells were counted. Cell damage was evaluated by lactate dehydrogenase (LDH)-releasing assay according as the manufacturer's instructions (Roche, Penzberg, Germany). Cells cultured on a 48-well plate were treated by each procedure, and cell damage was evaluated after 6 hours. The most severe cell damage was obtained by treatment with 1% Triton X (Sigma-Aldrich) and was used as a positive control. Cells with no treatment were applied as negative controls. Cell damage was expressed as: % LDH of sample − LDH of negative control/LDH of positive control − LDH of negative control.

In Vivo Study

After obtaining the approval of Kagoshima University ethics committee, all animals were used humanely in strict compliance with the ARVO Statement for the Use of Animals in Ophthalmic and Vision Research.

New Zealand albino rabbits (male; age, 14 weeks; weight, 3000 g; KBT Oriental Co., Saga, Japan) were first anesthetized with intramuscular injection of ketamine hydrochloride (14 mg/kg) and xylazine hydrochloride (14 mg/kg). Plasmid 10 μL mixed with PBS 2 μL was injected under surgical microscopy into the center of each cornea using a syringe with a 30-gauge needle. Immediately thereafter, a 6-mm US probe was placed directly on the corneal surface, and US was generated. When MBs were used, plasmid 10 μL mixed with perflutren protein (Optison; Amersham Health) 2 μL was injected instead of a plasmid with PBS. The intensity of US was set at 1 MHz, 120 seconds, 50% duty cycle, and 3 US powers—1 W/cm^2, 1.5 W/cm^2, and 2 W/cm^2—were examined.

GFP Expression. The presence of fluorescence signaling in the in vivo gene expression was determined using direct stereomicroscopy 72 hours after gene transfer (Olympus, Tokyo, Japan). The value of gene transfer was graded according to our scoring system by 3 masked observers. Only GFP expression scores agreed to by at least 2 of the observers were used in the analysis. Scoring criteria and representative photographs are shown in Figure 1. Transfection efficiency was expressed by a score of 0 to 5 (0 = not GFP positive; 5 = most intensely GFP positive).

Histology. All the animals were killed by overdose intravenous injection of pentobarbital. The eyes were enucleated 48 hours after treatment and were immediately frozen in liquid N2-cooled isopentane. Serial sections (6 μm) were sliced with a cryostat, placed on slides, and air dried. Regular fluorescent images and differential interference images were obtained by fluorescence microscopy (BX-FLA; Olympus, Tokyo, Japan) and were fitted using the IP Laboratory program (Scanalytics, Inc.; Fairfax, VA) on a personal computer. For light microscopy, the eyes were fixed with 3.7% formaldehyde in PBS, dehydrated with a graded alcohol series, and embedded in paraffin. Sections were cut and stained with hematoxylin and eosin. For the electron microscopy, the tissue was fixed with 4% paraformaldehyde, and the specimens were then dehydrated in a series of graded ethanols and embedded in epoxy resin. Thin sections were cut on an ultramicrotome, stained with uranyl acetate-lead citrate, and observed with an electron microscope (JEM-100CX; JEOL, Tokyo, Japan), as described. All the specimens were then observed by 2 masked observers who received no information about the specimens.

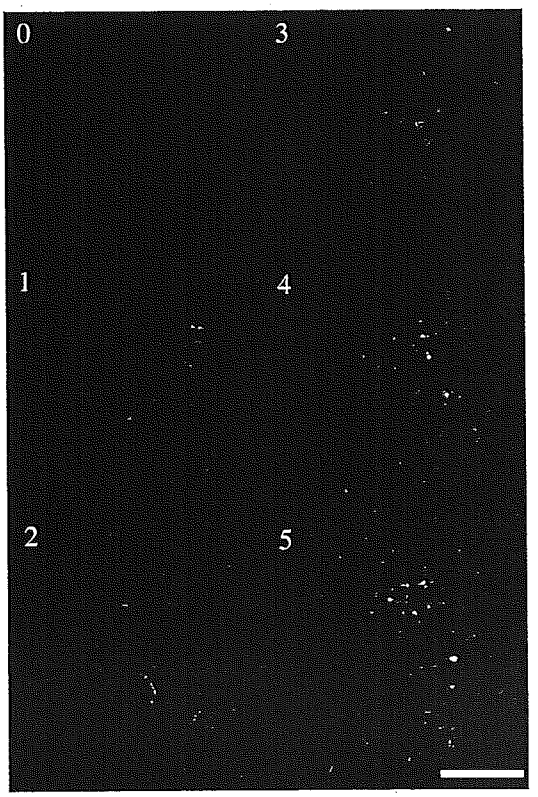

FIGURE 1. Representative photographs of scoring criteria. Gene transfer efficiency was expressed as a score of 0 to 5. Scoring was performed by 3 masked observers according to the following criteria. 0: no positive cells; 1: 1 to 25 positive cells in each field; 2: 26 to 50 positive cells in each field; 3: 51 to 75 positive cells in each field; 4: 75 to 150 positive cells in each field; 5: 151 or more positive cells in each field. Bar, 400 μm.

Statistical Analysis

All values were expressed as mean ± SEM. Analysis of variance with subsequent Scheffe test and Mann-Whitney U test was used to determine the significance of the difference in multiple comparison. Differences with a $P < 0.05$ were considered significant.

Results

In Vitro Study

Gene Transfer by Ultrasound. Numerous RC-1 cells were GFP positive after US exposure with the plasmid solution (Fig. 2A). Cells treated with the plasmid solution alone or the plasmid solution with MB perflutren protein (Optison; Amersham Health) alone did not show any fluorescein (Fig. 2B).

Gene Transfer by US Plus MBs. Under any of the following experimental US conditions—1 W/cm^2, 60 seconds, duty cycle 50%; 1 W/cm^2, 120 seconds, duty cycle 50%; 2 W/cm^2, 60 seconds, duty cycle 50%; 2 W/cm^2, 120 seconds, duty cycle 50%—the ratio of GFP-positive cells treated by US with MBs was significantly (two to four times) higher than that by US alone (Mann-Whitney U test, $P < 0.01$ Fig. 2C). To identify the optimal conditions to transfer genes by US plus MBs, the following four parameters were examined.

Duty Cycle. According to our previous studies, three duty cycles (20%, 50%, or 100%) were examined under an intensity of 1 W/cm^2 and 60-second exposure with 20% MBs.[29,30,32] As a result, the GFP-positive cell ratios were 11.3% with a duty cycle of 20%, 18.0% with a duty cycle of 50%, and 35.6% with a duty cycle of 100%. The GFP-positive cell ratio of duty cycle 100% US plus MBs was significantly higher than that under the other three conditions (Scheffe test, $P < 0.01$; Fig. 3A). On the other hand, the average number of survival cells was low with a duty cycle of 100%; for 79 cells per field, the duty cycle was 20%; for 171 cells per field, it was 50%; for 17.1 cells per field per, it was 100%. Cell damage was high in US, with a duty cycle of 20% or 100% in LDH assay (Fig. 3B). These results indicate that a duty cycle of 50% is preferable for obtaining high gene transfer efficiency with minimal cell damage.

MBs. Three concentrations of MBs—20%, 50%, and 100%—were examined under the US condition of 1 W/cm^2, 60 seconds, and duty cycle 50%. The GFP-positive ratio was highest in cells treated by US with 20% MBs (Scheffe test, $P < 0.01$; Fig. 3C). Cell survival was lowest in the 100% MB group, and no significant difference was found between the 20% and the 50% MB groups (170.7 cells/field in 20% MBs, 163 cells/field in 50% MBs, 38 cells/field in 100% MBs). A similar tendency was found by LDH assay (data not shown). Thus, 20% MBs was preferable.

Exposure Time. According to our previous study, a US exposure duration exceeding 120 seconds significantly damaged cells[29,32]; thus, a US exposure time of 15 to 120 seconds was examined under the condition of 1 W/cm^2, duty cycle 50%, with 20% MBs. As a result, the GFP-positive ratio was equally high for 60-and 120-second exposures (Fig. 3D). Cell damage was not apparent in any experimental group (Fig. 3E).

US Intensity. US intensities of 0.5, 1.0, 1.5, and 2.0 W/cm^2 were examined under the condition of 50% duty cycle and 60-second exposure with 20% MBs. A GFP-positive ratio of 0.5 W/cm^2 US group was significantly smaller than that in any of the other 3 groups (Scheffe test, $P < 0.01$; Fig. 2F). LDH assay also indicated that cell damage was significantly high in the 1.5 and 2.0 W/cm^2 exposure groups ($P < 0.01$; Fig. 3G), whereas little cell damage was observed in cells treated with 0.5 or 1.0 W/cm^2 US intensity. Representative images are shown in Figures 3H and 3I.

In Vivo Study

Gene Transfer by US. All GFP-positive cells in rabbit eyes underwent treatment. Eyes that received plasmid injection alone showed mild GFP-positive cells distributed within the injected area. GFP-positive cells were observed mainly in the corneal stroma. Average fluorescein score was 2.1 ($n = 24$). On the other hand, eyes that received plasmid injection and US (1 W/cm^2, 120 seconds, duty cycle 50%) had more GFP-positive cells (average score, 2.6; $n = 14$) than those that received plasmid injection alone. However, the difference was not statistically significant (Fig. 4).

Gene Transfer by US and MBs. From the in vitro study, 20% MBs were chosen. The average score of GFP-positive cells in cornea was 3.5 for eyes treated by US of 1 W/cm^2, 120 seconds, 50% duty cycle with MBs ($n = 41$). A significantly higher score (4.5) was obtained with simultaneous treatment by US and MBs than by US alone (2.6) or MBs alone (2.0) (Scheffe test, $P < 0.05$; Fig. 4), and it was achieved with US of 2 W/cm^2, 120 seconds, and 50% duty cycle ($n = 12$). GFP-

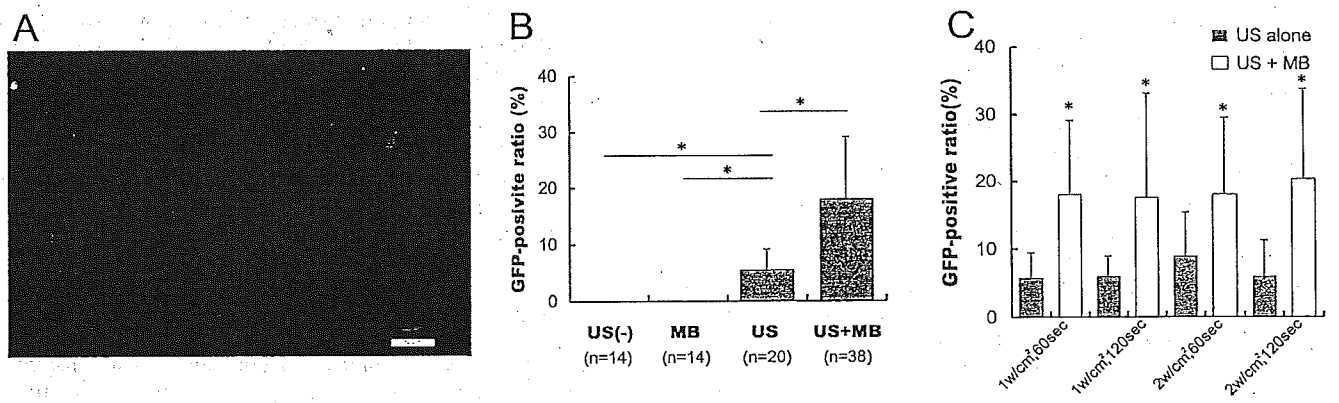

FIGURE 2. GFP-positive cells in gene-transferred rabbit corneal epithelial (RC-1) cells. (A) Fluorescence photograph of gene-transferred RC-1 cells. Many cells show a GFP-positive reaction in the whole cytoplasm. Bar, 100 μm. (B) GFP-positive ratio by different methods. Numerous RC-1 cells were GFP positive after ultrasonic exposure with the plasmid solution. Cells treated with the plasmid solution alone or the plasmid solution with perflutren protein (Optison; Amersham Health) alone did not show any fluorescein (Mann-Whitney U test, $^*P < 0.01$). (C) GFP-positive ratio of cells treated by US exposure with MBs. GFP-positive ratio treated by US with MBs was significantly higher (2–4 times) than that by US alone (Mann-Whitney U test, $^*P < 0.01$). 1 W/cm^2, 60 seconds, duty cycle 50%: US only, $n = 14$; with MB, $n = 38$. 1 W/cm^2, 120 seconds, duty cycle 50%: US only, $n = 15$; with MB, $n = 24$. 2 W/cm^2, 60 seconds, duty cycle 50%: US only, $n = 15$; with MB, $n = 23$. 2 W/cm^2, 120 seconds, duty cycle 50%: US only, $n = 15$; with MB, $n = 13$.

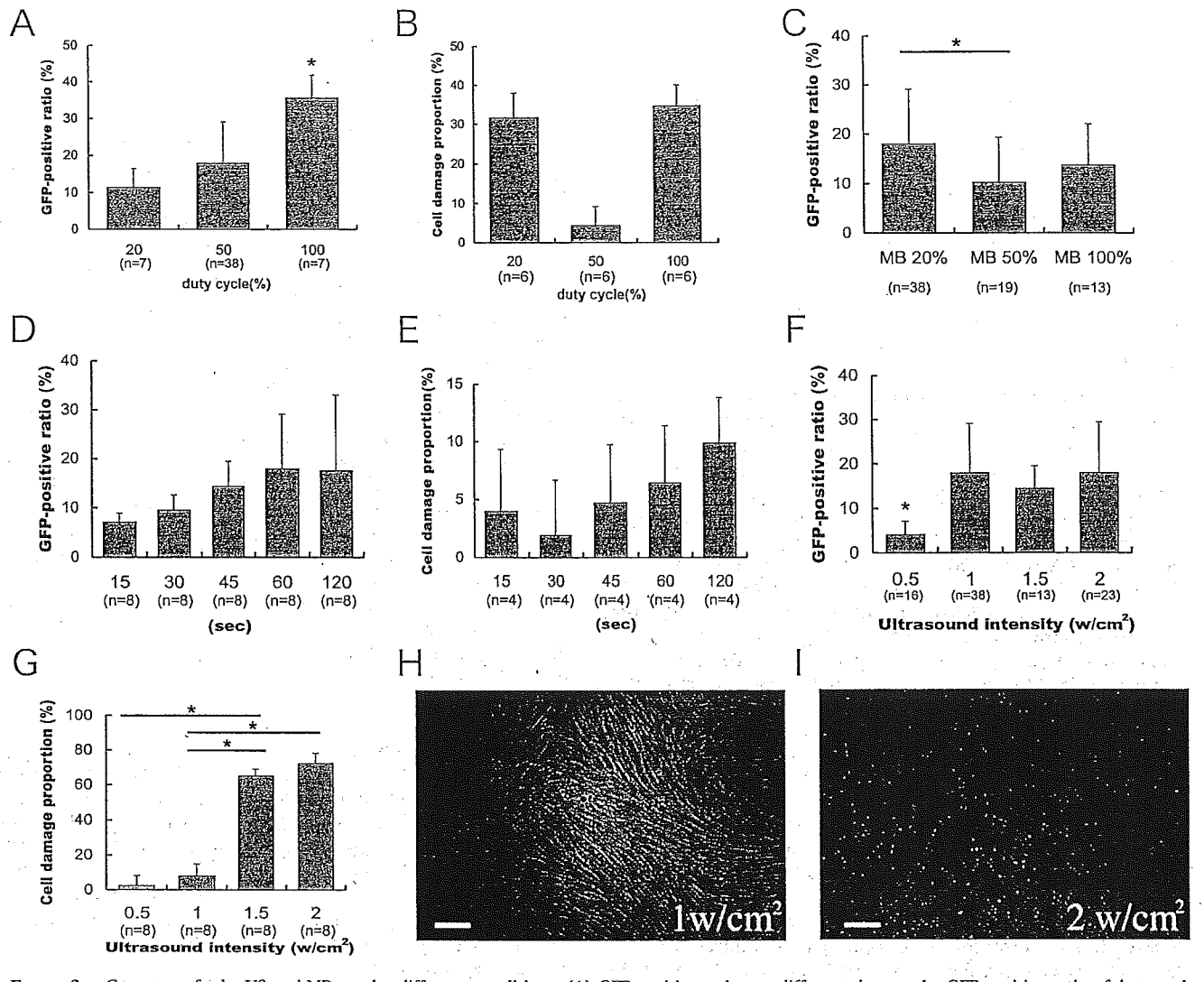

FIGURE 3. Gene transfer by US and MBs under different conditions. (A) GFP-positive ratio at a different duty cycle. GFP-positive ratio of duty cycle 100% US plus MBs was significantly higher than under the other 3 conditions (Scheffe test, $^*P < 0.01$). (B) Cell damage at different duty cycle. LDH assay indicates that cell damage was high in US at duty cycle 20% or 100%. (C) GFP-positive ratio at different concentrations of MBs. GFP-positive ratio was highest in cells treated by US with 20% MBs (Scheffe test, $^*P < 0.01$). (D) GFP-positive ratio at different US exposure times. GFP-positive ratio was equally high at 60- and 120-second exposures. (E) Cell damage at different US exposure times. Cell damage was not apparent in any experimental group. (F) GFP-positive ratio at different US powers. GFP-positive ratio of 0.5 W/cm^2 US group was significantly smaller than that of any of the other 3 groups (Scheffe test, $^*P < 0.01$). (G) Cell damage at different US powers. LDH assay indicates that cell damage was significantly high in the 1.5 or 2.0 W/cm^2 exposure group ($^*P < 0.01$), whereas little cell damage was noticed in cells treated with 0.5 or 1.0 W/cm^2 US power. (H) Phase-contrast photograph of RC-1 cells immediately after US exposure. No apparent cell damage was observed. Bar, 100 μm. (I) Phase-contrast photograph of RC-1 cells immediately after US exposure. Apparent cell damage was found in many cells (*arrows*). Bar, 100 μm.

positive cells were observed exclusively where US was exposed (Fig. 5). US intensity greater than 3 W/cm^2 caused immediate stromal haziness, which resolved spontaneously with no treatment (data not shown).

Duration of GFP Expression. The duration of GFP expression in cornea was evaluated in the eye treated with US and MBs under 20% MBs, 2 W/cm^2, 120 seconds, duty cycle 50%. GFP-positive cells appeared on the following day and increased the strength and the number of GFP-positive cells for 8 days (Fig. 6). GFP-positive cells in cornea gradually decreased in number and strength over time, and the average GFP-positive score on day 14 was 2 ($n = 13$) (Scheffe test $P < 0.01$). On day 30, only a faint GFP-positive reaction was noticed ($n = 4$).

Histologic Findings. Fluorescence microscopic examination showed that GFP was present in spindle-shaped cells in the targeted regions of the corneal stroma; thus, we speculated that keratocytes were also present (Fig. 7). Importantly GFP-positive cells were limited to the US-exposed area. No GFP was detected in untreated cornea or other intraocular tissues, such as ciliary epithelial cells, trabecular meshwork, cells lining Schlemm canal, lens epithelial cells, or retina (data not shown). Light and electron microscopic examination 48 hours after treatment showed no corneal damage, such as opacity or persistent epithelial defects, after US plus MB treatment, even under the strongest power studied in this series (2 W/cm^2, 120 seconds, duty cycle 100%; data not shown).

DISCUSSION

US is broadly used for clinical imaging, and its safety has been reliably established. Only in the past few years have studies demonstrated US-enhanced gene delivery to mammalian cells in vitro and in vivo.[12–18] Moreover, the presence of MBs near

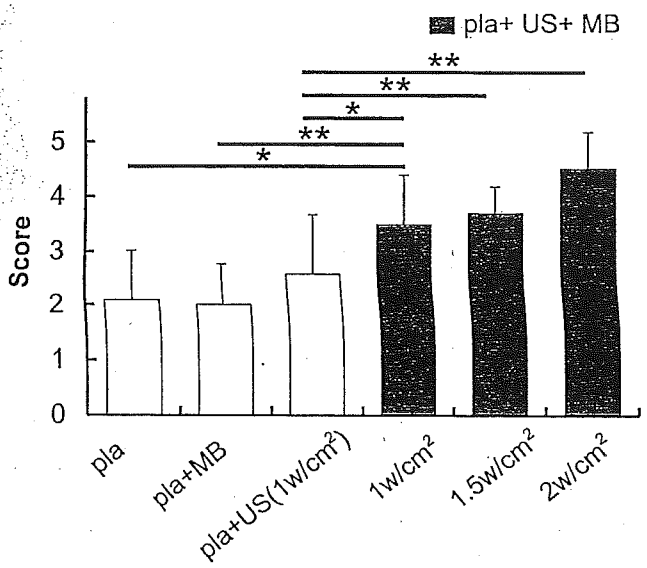

FIGURE 4. Gene transfer to rabbit cornea in vivo by US or MBs. Eyes that received plasmid injection alone or plasmid with MBs showed fluorescein-positive cells widely distributed within the injected area (plasmid alone, $n = 24$; plasmid with MB, $n = 8$). Eyes that received plasmid injection and US showed more numerous GFP-positive cells ($n = 14$) than those that received plasmid injection alone. A significantly higher score was obtained by simultaneous treatment of US and MBs (1 W/cm^2, $n = 41$; 1.5 W/cm^2, $n = 13$; 2 W/cm^2, $n = 12$) than by US alone (2.6) or MBs alone (2.0) (Scheffe test, $^*P < 0.05$, $^{**}P < 0.01$). Pla, plasmid DNA injection.

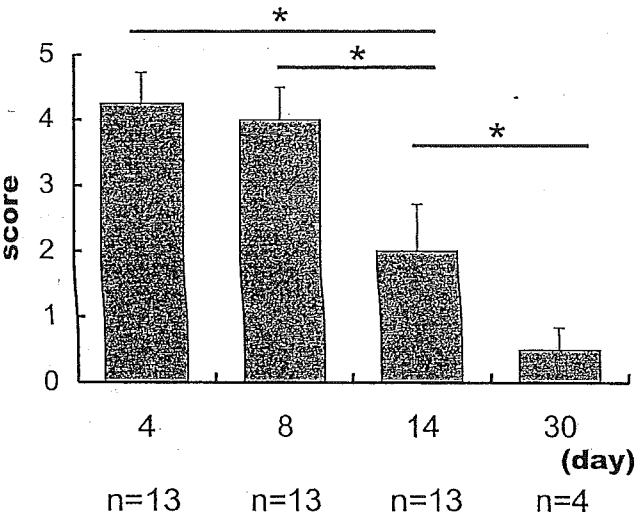

FIGURE 6. Duration of GFP expression in rabbit cornea was evaluated in the eye treated with US and MBs. GFP-positive cells appeared on the following day and increased the strength and number of GFP-positive cells for 8 days. GFP-positive cells in cornea gradually decreased in number and strength over time, and the average GFP-positive score on day 14 was 2 ($n = 13$) (Scheffe test, $^*P < 0.01$). On day 30, only faint GFP-positive reaction was observed ($n = 4$).

the cells further increases the gene transfection rate by lowering the acoustic pressure threshold needed to induce the microjets that penetrate the cellular membrane.[25-32] Sonography contrast-agent MBs with diameters ranging from 1 to 10 μm are considered ideal for this purpose. To gain further insight into the practicability of sonoporation, the cornea was selected as the subject of the present study because it can be noninvasively treated and monitored with the use of standard ophthalmological equipment, allowing visualization the cornea and the surrounding tissues under high magnification and per-

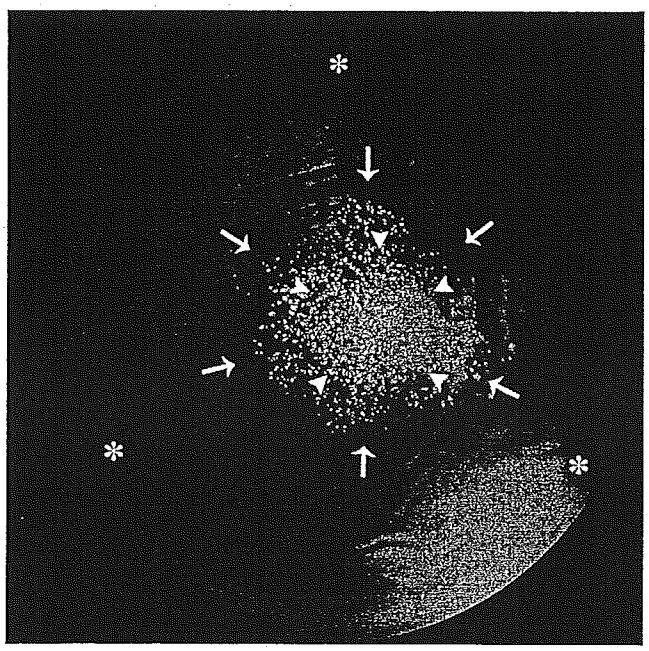

FIGURE 5. Fluorescence photograph of rabbit cornea 7 days after treatment. Twelve microliters plasmid with MBs was injected into the central cornea (*arrows*); this was followed by US exposure. *Arrowheads* indicate exactly where the US probe was placed. GFP-positive cells were specifically located where the US was exposed. A few GFP-positive cells are seen in the surrounding area. *Asterisks* indicate the corneal margin.

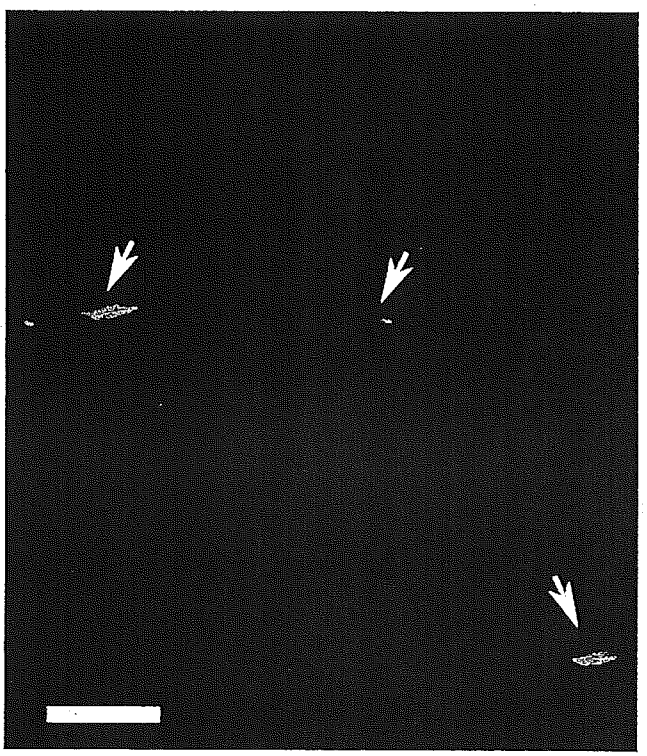

FIGURE 7. Fluorescence microscope photograph of rabbit cornea after treatment with US and MBs (2 W/cm^2, duty cycle 50%, 120 seconds). GFP is present mainly in spindle-shaped cells in the targeted regions of the corneal stroma (*arrows*). Bar, 10 μm.

mitting easy determination of gene transfection and tissue damage.

To establish the optimal condition of US MB-mediated gene transfer to cornea, 98 different patterns of various US conditions were examined in vitro in preliminary studies because it is difficult in practice to study so many different patterns using rabbit eyes in vivo. First, the duty cycle of US was evaluated. Results clearly showed that a duty cycle of 100% is most effective to transfer genes. However, cell damage was too strong with a duty cycle of 100%. Therefore, a duty cycle of 50% was chosen for our purpose. Second, the amount of MBs perflutren protein (Optison; Amersham Health) was evaluated. Cytotoxicity was highest in 100% MBs, and gene transfer efficiency was highest in 20% MBs. Thus, 20% MBs was chosen. Third, the exposure time of US was evaluated. An exposure time longer than 120 seconds significantly damaged the cells, and an exposure time shorter than 60 seconds could not transfer the gene efficiently. Sixty- and 120-second exposure provided almost identical gene transfer efficiency and cell toxicity. Finally, US power was studied. It is understandable that high US power can transfer the gene to cells but also induce strong cell damage. Considering gene transfer efficiency and cellular damage, a US power of 1 or 2 W/cm^2 should be appropriate.

Contrary to in vitro experiments, US alone revealed no significant enhancement of gene transfer compared with controls. Because the cornea is composed of multiple cell layers and abundant extracellular matrix, it is postulated that higher US intensities are needed to produce sufficient microjets to damage cells or inject genes into cells. Adding MB with the plasmids, on the other hand, increased gene transfer efficiency by twofold to threefold. Optic examination showed that GFP was present mainly in keratocytes at the US-targeted regions of the corneal stroma. GFP was not detected in the untreated area of the cornea or other intraocular tissues. It is noteworthy that US induced no immediate corneal damage, such as opacity or defect of corneal/ciliary epithelial cells. Surrounding trabecular meshwork, cells lining Schlemm canal, lens epithelial cells, and retina seemed to be intact.

Previously, Wang et al.[22] reported perflutren protein (Optison; Amersham Health) with DNA could achieve effective gene transfer in muscle. However, effective gene transfer could not be performed in cornea in the present study. Because the cornea has more abundant extracellular materials than muscle, perflutren protein (Optison; Amersham Health) alone might not be effective for transferring DNA to cells.

Viral vector- or liposome-mediated gene transfer methods are effective for transferring genes to almost every cell that comes in contact with vectors[33,34] (e.g., the adenoviral vector). Because the long-term effects of gene transfer on recipient cells remain unclear, the cells to which genes are transferred should be strictly controlled. Especially when transferring genes to the cornea, the pupillary area should be avoided so as not to threaten vision. The present method greatly reduces this concern because of the precise targeting it makes possible.

In previous studies we reported that electroporation-mediated gene transfer can be achieved in rat cornea.[35–37] However, in larger animals, including rabbit, electroporation may be hazardous because the cardiovascular system is sometimes impaired by treatment (data not shown). Therefore, at present it might not be easy to apply electroporation for human gene therapy.

When the vehicle with the gene of interest is injected into tissue through a local gene delivery method such as liposome or viral vector injection, the vehicle spreads in every direction three dimensionally. Accordingly, gene transfer is achieved three dimensionally in a similar way. However, in the treatment of a surface organ such as skin or cornea, two-dimensional gene transfer is sometimes preferable. Using the characteristics of ultrasound, the present method achieved two-dimensional gene transfer.

Thirty percent to 40% of the total corneal area was covered by a 12-μL plasmid injection. Gene transfer was achieved in the area exposed to US. To expand the area of gene transfer, it was necessary to improve the injection method and the US probe. The present method can be applied to a variety of purposes, such as making it feasible to use highly fragile proteins.[38,39] With the present method, we were able to superficially deliver genes to a targeted tissue surface area two dimensionally. Thus, this sonoporation method could become a valuable modality for therapy and research that require surface-localized drug delivery or gene induction.[40]

Many questions remain before the present method can be applied clinically. The optimal US condition required for efficient gene transfer is highly dependent on the tissue, and the biologic structures responsible for the US effect vary greatly among species. These issues must be carefully explored. Of necessity, there is another limitation to the present study. We examined a rabbit corneal epithelial cell line in an the vitro study, but the gene-transferred cells were mainly keratocytes in the in vivo study. In our preliminary study, rabbit keratocytes were cultured; however, the morphology of these cells soon changed and differentiated into unidentifiable cells. Therefore, we used the rabbit corneal cell line RC-1.

To summarize, our studies show that using US in conjunction with commercially available MBs can enhance gene delivery to cells without damaging tissues. Although this modality was highly dependent on acoustic conditions and bubble concentration, its simplicity and noninvasiveness may provide a new avenue for microinjecting various substances into a wide range of living tissues.

References

1. Marshall E. Gene therapy's growing pains. *Science.* 1995;269:1050, 1052–1055.
2. Felgner PL, Barenholz Y, Behr JP, et al. Nomenclature for synthetic gene delivery systems. *Hum Gene Ther.* 1997;8:511–512.
3. Marshall E. Gene therapy death prompts review of adenovirus vector. *Science.* 1999;286:2244–2245.
4. Hacein-Bey-Abina S, Le Deist F, Carlier F, et al. Sustained correction of X-linked severe combined immunodeficiency by ex vivo gene therapy. *N Engl J Med.* 2002;346:1185–1193.
5. Grisham J. Inquiry into gene therapy widens. *Nat Biotechnol.* 2000;18:254–255.
6. Wolff JA, Malone RW, Williams P, et al. Direct gene transfer into mouse muscle in vivo. *Science.* 1990;247:1465–1468.
7. Wolff JA, Ludtke JJ, Acsadi G, Williams P, Jani A. Long-term persistence of plasmid DNA and foreign gene expression in mouse muscle. *Hum Mol Genet.* 1992;1:363–369.
8. Felgner PL, Gadek TR, Holm M, et al. Lipofection: a highly efficient, lipid-mediated DNA-transfection procedure. *Proc Natl Acad Sci USA.* 1987;84:7413–7417.
9. Stechschulte SU, Joussen AM, von Recum HA, et al. Rapid ocular angiogenic control via naked DNA delivery to cornea. *Invest Ophthalmol Vis Sci.* 2001;42:1975–1979.
10. Nishi T, Yoshizato K, Yamashiro S, et al. High-efficiency in vivo gene transfer using intraarterial plasmid DNA injection following in vivo electroporation. *Cancer Res.* 1996;56:1050–1055.
11. Drabick JJ, Glasspool-Malone J, King A, Malone RW. Cutaneous transfection and immune responses to intradermal nucleic acid vaccination are significantly enhanced by in vivo electropermeabilization. *Mol Ther.* 2001;3:249–255.
12. Newman CM, Lawrie A, Brisken AF, Cumberland DC. Ultrasound gene therapy: on the road from concept to reality. *Echocardiography.* 2001;18:339–347.

13. Kim HJ, Greenleaf JF, Kinnick RR, Bronk JT, Bolander ME. Ultrasound-mediated transfection of mammalian cells. *Hum Gene Ther.* 1996;7:1339-1346.
14. Bao S, Thrall BD, Miller DL. Transfection of a reporter plasmid into cultured cells by sonoporation in vitro. *Ultrasound Med Biol.* 1997;23:953-959.
15. Wyber JA, Andrews J, D'Emanuele A. The use of sonication for the efficient delivery of plasmid DNA into cells. *Pharm Res.* 1997;14: 750-756.
16. Miller DL, Williams AR, Morris JE, Chrisler WB. Sonoporation of erythrocytes by lithotripter shockwaves in vitro. *Ultrasonics.* 1998;36:947-952.
17. Lawrie A, Brisken AF, Francis SE, et al. Ultrasound enhances reporter gene expression after transfection of vascular cells in vitro. *Circulation.* 1999;99:2617-2620.
18. Manome Y, Nakamura M, Ohno T, Furuhata H. Ultrasound facilitates transduction of naked plasmid DNA into colon carcinoma cells in vitro and in vivo. *Hum Gene Ther.* 2000;11:1521-1528.
19. McDonnell PJ. Excimer laser corneal surgery: new strategies and old enemies. *Invest Ophthalmol Vis Sci.* 1995;36:4-8.
20. Seitz B, Baktanian E, Gordon EM, Anderson WF, LaBree L, McDonnell PJ. Retroviral vector-mediated gene transfer into keratocytes: in vitro effects of polybrene and protamine sulfate. *Graefes Arch Clin Exp Ophthalmol.* 1998;236:602-612.
21. Bennett J, Maguire AM. Gene therapy for ocular disease. *Mol Ther.* 2000;1:501-505.
22. Wang X, Liang HD, Dong B, Lu QL, Blomley MJ. Gene transfer with microbubble ultrasound and plasmid DNA into skeletal muscle of mice: comparison between commercially available microbubble contrast agents. *Radiology.* 2005;237:224-229.
23. Greenleaf WJ, Bolander ME, Sarkar G, Goldring MB, Greenleaf JF. Artificial cavitation nuclei significantly enhance acoustically induced cell transfection. *Ultrasound Med Biol.* 1998;24:587-595.
24. Lu QL, Bou-Gharios G, Partridge TA. Non-viral gene delivery in skeletal muscle: a protein factory. *Gene Ther.* 2003;10:131-142.
25. Blomley M. Which US microbubble contrast agent is best for gene therapy? *Radiology.* 2003;229:297-298.
26. Lawrie A, Brisken AF, Francis SE, Cumberland DC, Crossman DC, Newman CM. Microbubble-enhanced ultrasound for vascular gene delivery. *Gene Ther.* 2000;7:2023-2027.
27. Shohet RV, Chen S, Zhou YT, et al. Echocardiographic destruction of albumin microbubbles directs gene delivery to the myocardium. *Circulation.* 2000;101:2554-2556.
28. Unger EC, Hersh E, Vannan M, McCreery T. Gene delivery using ultrasound contrast agents. *Echocardiography.* 2001;18:355-361.
29. Taniyama Y, Tachibana K, Hiraoka K, et al. Local delivery of plasmid DNA into rat carotid artery using ultrasound. *Circulation.* 2002;105:1233-1239.
30. Taniyama Y, Tachibana K, Hiraoka K, et al. Development of safe and efficient novel nonviral gene transfer using ultrasound: enhancement of transfection efficiency of naked plasmid DNA in skeletal muscle. *Gene Ther.* 2002;9:372-380.
31. Lu QL, Liang HD, Partridge T, Blomley MJ. Microbubble ultrasound improves the efficiency of gene transduction in skeletal muscle in vivo with reduced tissue damage. *Gene Ther.* 2003;10:396-405.
32. Nakashima M, Tachibana K, Iohara K, Ito M, Ishikawa M, Akamine A. Induction of reparative dentin formation by ultrasound-mediated gene delivery of growth/differentiation factor 11. *Hum Gene Ther.* 2003;14:591-597.
33. Vincent MC, Trapnell BC, Baughman RP, Wert SE, Whitsett JA, Iwamoto HS. Adenovirus-mediated gene transfer to the respiratory tract of fetal sheep in utero. *Hum Gene Ther.* 1995;6:1019-1028.
34. Porada CD, Tran N, Eglitis M, et al. In utero gene therapy: transfer and long-term expression of the bacterial neo(r) gene in sheep after direct injection of retroviral vectors into preimmune fetuses. *Hum Gene Ther.* 1998;9:1571-1585.
35. Oshima Y, Sakamoto T, Hisatomi T, et al. Targeted gene transfer to corneal stroma in vivo by electric pulses. *Exp Eye Res.* 2002;74: 191-198.
36. Oshima Y, Sakamoto T, Hisatomi T, Tsutsumi C, Ueno H, Ishibashi T. Gene transfer of soluble TGF-beta type II receptor inhibits experimental proliferative vitreoretinopathy. *Gene Ther.* 2002;9: 1214-1220.
37. Sakamoto T, Oshima Y, Nakagawa K, Ishibashi T, Inomata H, Sueishi K. Target gene transfer of tissue plasminogen activator to cornea by electric pulse inhibits intracameral fibrin formation and corneal cloudiness. *Hum Gene Ther.* 1999;10:2551-2557.
38. Tachibana K, Tachibana S. Transdermal delivery of insulin by ultrasonic vibration. *J Pharm Pharmacol.* 1991;43:270-271.
39. Tachibana K, Uchida T, Ogawa K, Yamashita N, Tamura K. Induction of cell-membrane porosity by ultrasound (Letter). *Lancet.* 1999;353:1409.
40. Tachibana K, Tachibana S. The use of ultrasound for drug delivery. *Echocardiography.* 2001;18:323-328.

Cellular and Molecular Biology™ **51**, Online, OL767-OL784
DOI 10.1170/91

ISSN 1165-158X
2005 Cell. Mol. Biol.™

Review

TRANSDERMAL DRUG DELIVERY USING ULTRASOUND – THEORY, UNDERSTANDING AND CRITICAL ANALYSIS

M. SIVAKUMAR[1✉], K. TACHIBANA[2], A.B. PANDIT[3], K. YASUI[1], T. TUZIUTI[1], A. TOWATA[1] and Y. IIDA[1]

[1✉] Ultrasonic Processing Group, National Institute of Advanced Industrial Science and Technology (AIST), 2266-98 Anagahora, Shimoshidami, Moriyama-ku, Nagoya 463-8560, Japan
Fax: +81 52 736 7400; E-mail: manickam-sivakumar@aist.go.jp; siva_chem@yahoo.com
[2] Department of Anatomy, School of Medicine, Fukuoka University, 7-45-1 Nanakuma, Jonan-ku, Fukuoka 814-0180, Japan
[3] Chemical Engineering Division, University Institute of Chemical Technology (UICT), Matunga, Mumbai, 400 019, India

Received January 31, 2005; Accepted May 24, 2005; Published September 2, 2005

Abstract - This review focuses on a unique transdermal drug delivery enhanced by the action of ultrasound, referred as sonophoresis. Sonophoresis is an active form of transdermal delivery which enhances the transport of permeants, such as drugs through cell membranes as a result of ultrasonic energy. Ultrasonic sound waves cause acoustic cavitation, the resultant effects of which microscopically disrupt the lipid bilayers of the stratum corneum and thereby influencing the influx of permeants. Sonophoresis increases the penetration of various low molecular weight drugs as well as high molecular weight proteins. The objective of this review is to account the role of ultrasound parameters and the associated cavitational effects, gained through a number of investigations, in order to facilitate the understanding of this method.

Key words: Acoustic cavitation, transdermal, drug delivery, ultrasound, sonophoresis, skin penetration, sonochemical

INTRODUCTION

Drug delivery techniques were established to deliver or control the amount, rate and sometimes targeting of the drugs to specific body organs in order to optimize its therapeutic effect, patient convenience and dose. Intravenous injection and oral dosing, the two modes of drug delivery in popular use today, have many shortcomings. The recent development of biotechnology drugs based on macromolecules, particularly polypeptide drugs such as interferons and erythropoietin, are a key factor in the growth of the drug-delivery market. Approximately 40 macromolecule drugs are currently being marketed, generating estimated worldwide sales of $20 billion. It is estimated that 400 additional macromolecule drugs are in clinical development. However, at this stage evidence supporting the clinical application of many of these drugs is limited. One reason for this is perhaps because oral administration of these drugs becomes impossible as these drugs break down quickly and are poorly absorbed into the bloodstream. Whereas, intravenous administration of these drugs with chronic application becomes inconvenient, time-consuming and known to result in poor patient-compliance (25). Therefore, the successfulness of new therapeutic biological drugs will depend on a novel technology to enable them to reach their target within the body. An appealing alternative to intravenous and oral drug delivery is "transdermal" or "through the skin" drug delivery, a powerful and a painless tool which avoids the problems inherent with the intravenous and oral delivery methods, with the added benefits of possible sustained controlled release and analyte extraction, for example extracting glucose and other constituents of interstitial fluid across permeabilised skin (21,86,87). These advantages of transdermal systems make them very promising for drug delivery.

Abbreviations: atm: atmosphere; **Hz**: hertz; **J**: joule; **J/cm²**: joules per square centimeter; **K/sec**: kelvin per second; **kHz**: kilohertz; **MHz**: megahertz; **m/s**: meters per second; **mA/cm²**: milliamperes per square centimeter; **nm**: nanometer; **Pa**: pascal; **SC**: stratum corneum; **W/cm²**: watts per square centimeter

Why transdermal drug delivery?

As the body's largest organ, skin is a promising target of drug delivery. However, skin is an extremely effective barrier membrane - perhaps the most effective barrier membrane (40) for the human organism. The skin's

outermost layer, the stratum corneum (SC) represents an impenetrable barrier to molecular transport and thus to most of the drugs from entering the body through the skin.

The stratum corneum is of 10-15 μm in thickness, and is composed of dead keratin-rich cells (corneocytes) and a lipid matrix. The intercellular space is an ordered, impermeable bilayer structure of lipid and aqueous layers, along with fatty acids and cholesterols. Thus, due to the structure and composition, the stratum corneum is almost impermeable.

Three possible pathways, transappendageal, transcellular, and intercellular have been suggested for molecular transport through the SC (110). The transappendageal pathway is primarily through hair follicles. However, the transappendageal skin transport in humans is limited by the small surface area available. The fractional area of hair follicles relative to the skin area is 10^{-2}-10^{-5} (111). The transcellular pathway requires the substrates to travel through the corneocytes while the intercellular pathway is via the extracellular matrix between the corneocytes. For intercellular skin transport, hydrophilic substrates are rate limited by the lipid environment of the intercellular matrix of the SC (1). On the other hand, lipophilic substrates partition into the intercellular lipids of the SC. However, the rate-limiting step is the partition into the epidermis, which is practically an aqueous environment. Molecular transport through the skin has been described by a solubility-diffusion model (102) and a transfer free energy model (103). Skin penetration also depends on anatomical site, age, sex, skin care, hydration and temperature (75). In addition, the molecular weight (MW) of the substrate affects percutaneous absorption. The diffusion through the SC follows the expression $Da\ (MW)^{-b}$ where the value of b varies between 0.3 and 0.6 (41).

As a result, the stratum corneum is the rate-determining barrier to percutaneous absorption of most compounds. If a molecule can cross the stratum corneum and the epidermis, it can then reach the dermis and potentially be absorbed by the skin's blood vessels. Fig. 1 shows the structure of human skin and its components and Fig. 2 provides the structure of stratum corneum (27).

Transdermal drug delivery thus involves passive diffusion of a drug substance through the skin and subsequent absorption by the capillary system for systemic distribution. Presently available transdermal patches can be classified into four categories on the basis of their

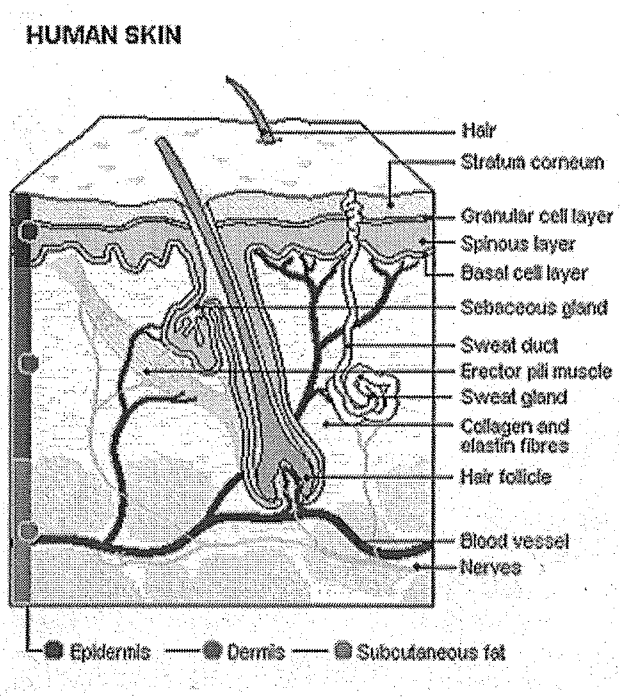

Fig. 1 Structure of human skin and its components

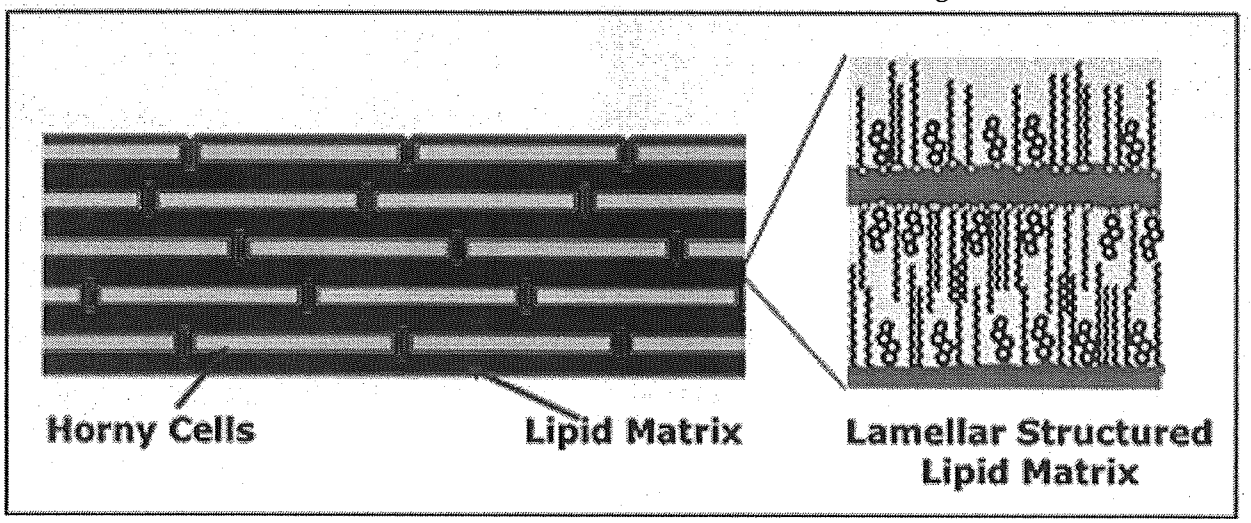

Fig. 2 Structure of stratum corneum

design: single-layer-drug-in adhesive, multi-layer-drug-in adhesive, reservoir and matrix patches (147). The basic components of these patches are impermeable backing, rate-controlling membrane, liner, adhesive and the drug. These patches can be placed on the arm, on the back, or anywhere that is discreet and effective. Transdermal patches are engineered with safety, security, effectiveness and comfort in mind. Except very few cases, where there are mild skin irritations that occur at the site of the patch application, transdermal patches are a great way to avoid side effects, since a patch's ingredients do not enter the digestive system, therefore, the chance of getting an upset stomach is small (149).

The commercialization of transdermal patches for controlled drug delivery began two decades ago and has resulted in diverse products. There are a number of medications that are available in patch form today and the technology has a proven record of FDA approval. Since the first transdermal patch was approved in 1981 to prevent the nausea and vomiting associated with motion sickness, the FDA has approved, throughout the past 24 years, more than 35 transdermal patch products, spanning 13 molecules (146,148) which are Nitroglycerine for angina, Scopolamine for motion sickness treatment, Fentanyl for pain control, Nicotine for smoking cessation, Estrogen for hormone replacement therapy, Testosterone for male hypogonadism, Clonidine for hypertension treatment, Lidocaine and Prilocaine for topical anaesthesia, Ethinylestradiol and Norelgestromin for contraception, Norethindrone to help reducing the overgrowth of the lining of the uterus and Oxybutynin for overactive bladder.

Although the transdermal approach has many advantages, but, yet this approach has not developed as widely as was once predicted. This is due to that current transdermal patch designs are not capable of transporting large molecular drug through the skin barrier, especially peptides and proteins (of molecular weight more than 500 Da, for example, insulin - 6000 Da), which includes many drugs that are marketed or will emerge from the biotechnology industry. The reason, as mentioned earlier, is due to the difficult-to-cross stratum corneum. The physiochemical nature of this pathway dictates that only lipophilic drugs such as estradiol ($\log K_{o/w} = 2.58$) will readily diffuse through stratum corneum. In addition, the main disadvantage of traditional transdermal delivery is that therapeutic plasma levels are obtained very slowly (6 to 8 hr after application in the case of scopolamine) (107).

Techniques to enhance transdermal drug delivery

Transdermal delivery of drugs of much higher molecular weight (>500 Da) thus requires skin permeation enhancement mechanisms. In the quest to facilitate and increase the rate of delivery of higher molecular weight drugs through epidermis, several avenues have been proposed. These include the use of chemical enhancers (7,24,25,118,137,139), iontophoresis (7,18,35,108,142), electroporation (25,34,99,104,105), microneedles (7,148), laser ablation (49,64,95), pressure waves or shock waves (28,53), magnetic field (magnetophoresis) (57,94,109), photomechanical waves (60-62,76,77) and RF ablation (151).

– *Chemical enhancers*: Numerous compounds have been evaluated as chemical enhancers for penetration enhancing activity, including sulphoxides (such as dimethyl-sulphoxide, DMSO), azones (e.g. laurocapram), pyrrolidones (for example 2-pyrrolidone, 2P), alcohols and alkanols (ethanol or decanol), glycols (for example propylene glycol, PG, a common excipient in topically applied dosage forms), surfactants (also common in dosage forms) and terpenes (139). Using a chemical enhancer, for example, nerolidol (a terpene) has been shown to enhance 5-fluorouracil permeability over 20-fold through human skin *in vitro* (24). These chemical enhancers temporarily alter the barrier properties of the stratum corneum that enhances the drug flux (7,118). However, due to the incredibly slow permeability coefficients of the macromolecules, the enhancement effects required to ensure the delivery of pharmacologically effective concentrations are likely to beyond the capability of chemical enhancers tolerated by the skin (25).

– *Iontophoresis*: This method is about a century old technique and refers to the facilitated movement of ions of soluble salts through the application of a small electric current (usually 0.5 mA/cm^2) in order to drive the solute molecules into the skin (108). The effect of simple electrorepulsion is known to be one of the main mechanisms by which iontophoresis produces its enhancement effects, though other factors including the increased permeability of the stratum corneum by the generation of small pores (142) in the presence of a flow of an electric current and electroosmosis of uncharged and larger water soluble molecules are also possible (7). There have been numerous research applications of iontophoresis in topical drug delivery for lower molecular weight solutes (<500 Da) (7,108). Iontophoresis using specially designed current can give about 400 % better penetration compared to simple topical application (35).

– *Electroporation*: Electroporation is a mechanical method used to introduce macromolecules into a host cell through the cell membrane. In this procedure, application of a large electric pulse (10 μs-100 ms) temporarily disturbs the phospholipid bilayer and causes the formation of transient pores in the membrane, allowing macromolecules like DNA to pass into the cell. Prausnitz and Weaver and Preat have done intensive work for enhancing the transdermal drug delivery using this technique (104). The electrical resistance of the skin is reported to drop as much as three orders of magnitude within microseconds of administration of an

electrical pulse (99,105). Increases in transdermal penetration of up to 104-fold have been reported *in vitro* for various sizes of molecules. To date there appear to be no clinical studies assessing the ability of the technique to facilitate transdermal drug delivery (25).

– *Microneedles*: A newer and potentially more promising technology for macromolecule delivery is microneedle-enhanced delivery. These systems use an array of tiny needle-like structures to open pores in the stratum corneum and facilitate drug transport. The structures are small enough that they do not penetrate into the dermis and thus do not reach the nerve endings, so there is no sensation of pain. The structures can be either solid (serving as a pre-treatment prior to patch application), solid with drug coated directly on the outside of the needles, or hollow to facilitate fluidic transport through the needles and into the lower epidermis. These systems have been reported to greatly enhance (up to 100,000-fold) the permeation of macromolecules through skin (7,148).

– *Laser ablation*: The use of lasers to remove the stratum corneum barrier by controlled ablation (49) has also been investigated as a means of enhancing topical drug delivery. In 1991, Nelson *et al.* (95) reported that mid-infrared laser (1 J/cm^2) ablation of pig stratum corneum enhanced the permeation of both hydrocortisone and interferon. Lee *et al.* (64) found that stratum corneum ablation with low intensity (0.35-0.45 J; 0.91-1.17 J/cm^2) erbium:yttrium-aluminum-garnet (YAG) laser (light emission at 2940 nm) increased the permeability of both lipophilic and hydrophilic drugs through nude mouse skin *in vitro*. However, the structural changes caused by this technique still need to be assessed for safety and reversibility, particularly at the higher intensities that may be needed to enhance the penetration of large molecular weight solutes where evidence of deeper level ablation effects exist (64).

– *Pressure waves or shock waves*: Pressure waves, which are generated by intense laser radiation, can permeabilize the stratum corneum (SC) as well as the cell membrane. These pressure waves are compression waves and thus exclude biological effects induced by cavitation. Their amplitude is in the hundreds of atmospheres (bar) while the duration is in the range of nanoseconds to a few microseconds. The pressure waves interact with cells and tissue in ways that are probably different from those of ultrasound. Furthermore, the interactions of the pressure waves with tissue are specific and depend on their characteristics, such as peak pressure, rise time and duration. A single pressure wave is sufficient to permeabilize the SC and allow the transport of macromolecules into the epidermis and dermis. Cell permeabilization using these waves may be a way of introducing macromolecules and small polar molecules into the cytoplasm, and may have applications in gene therapy and anticancer drug delivery. In addition, drugs delivered into the epidermis can enter the vasculature and produce a systemic effect. For example, insulin delivered by pressure waves resulted in reducing the blood glucose level over many hours. The application of pressure waves does not cause any pain or discomfort and the barrier function of the SC always recovers (28).

Kodama and co-workers argued that shock waves permeabilize membrane by inducing relative displacement between the cell and the surrounding fluid (53). They have used three different shock-wave sources for the generation of these waves; argon fluoride excimer laser, ruby laser, and shock tube. The uptake of two fluorophores, calcein (MW: 622 Da) and fluorescein isothiocyanate (FITC) - dextran (MW: 71,600 Da), into HL-60 human promyelocytic leukemia cells was investigated. The intracellular fluorescence was measured by a spectrofluorometer, and the cells were examined by confocal fluorescence microscopy. A single shock wave generated by the shock tube delivered both fluorophores into approximately 50 % of the cells (p, 0.01), whereas shock waves from the lasers did not. The cell survival fraction was 0.95. Confocal microscopy showed that, in the case of calcein, there was a uniform fluorescence throughout the cell, whereas, in the case of FITC-dextran, the fluorescence was sometimes in the nucleus and at other times not. They concluded that the impulse of the shock wave (i.e. the pressure integrated over time), rather than the peak pressure, was a dominant factor for causing fluorophore uptake into living cells, and that shock waves might have changed the permeability of the nuclear membrane and transferred molecules directly into the nucleus.

– *Magnetophoresis*: Limited work probed the ability of magnetic fields to move diamagnetic materials through skin (57,94). Santini *et al.* (109) have discussed the interesting idea of employing intelligent systems based on magnetism or microchip technology to deliver drugs in controlled, pulsatile mode.

– *Photomechanical waves*: Photomechanical waves (PW's) are also known as laser generated stress waves. In this technique, a drug solution placed on the skin and covered by a black polystyrene target, is irradiated with a laser pulse. The resultant photomechanical wave stresses the horny layer and enhances drug delivery (60). The mechanism(s) by which PW's increase the permeability of the stratum corneum is not entirely clear. Microscopic studies have indicated that changes in the lacunar system are visible following exposure of human stratum corneum to a PW (77) and that expansion of this system is suggested to result in the formation of transient channels through the stratum corneum (76). The largest molecule that has been reported to be delivered through rat skin to date has been 40 kDa (61). Suggestion has been raised that many clinically important proteins such as insulin (6,000 Da) and hematopoietin (48,000 Da) are within, or close to, the delivery capability range of PW's (62), however, this relatively new technique

does not yet seem to have produced any human clinical data.
– *RF ablation*: This technique uses radio-frequency (RF) electrical current and creates microscopic passages in the stratum corneum and outer epidermis via a process called cell ablation. This technique is typically performed at frequencies above 100 kHz that do not stimulate the muscles and nerves. The pre-clinical and clinical trials using this technique for a variety of drugs, including hGH (a large 22 kDa protein), demonstrating high therapeutic drug delivery levels and excellent bioavailability (151).

In addition to the above methods, a number of other methods have also been studied for the transdermal delivery of various drugs. Thermal poration, an approach that has been used to deliver conventional drugs (115) and vaccines (16) to animals and to extract interstitial fluid glucose from human being (38). High-velocity jet injectors are also receiving increased attention (46). Clinically insulin has been delivered using this technique (17). Jet injectors are presently on the market and a number of companies are developing new devices (106).

SONOPHORESIS

Apart from a few dermal patches, we have still not realized the enormous advantages of transdermal delivery over the traditional routes for giving drugs. In the continuous search of newer and efficient techniques, "sonophoresis" in recent years has become a promising approach and it has become the subject of many studies. Sonophoresis is similar to iontophoresis. However, the problem with iontophoresis is that it only works if the molecule can be ionised into positive and negative charged components. This is not an impediment for sonophoresis.

Sonophoresis is a transdermal drug delivery technology in which enhancement of the transport of permeants occurs by the application of ultrasound. Simply this process can be referred to as the use of the energy of sound waves in order to drive the movement (flux) of chemicals transcutaneously through the skin by means of changing the barrier properties of the skin (2,8,10,34). Passing intense ultrasound waves results in cavitation which is the main mechanism for sonophoretic enhancement.

Ultrasonic domain

It's necessary to understand what sound is before one can understand ultrasound. Sound is the propagation of pressure wave through some physical elastic medium. Usually the medium is air, but a liquid works well too. A vacuum doesn't. The longitudinal pressure waves are generated due to mechanical disturbances. Mechanical energy is being converted to a wave form that radiates energy away from the disturbance, transferring energy to the medium and to objects that the wave contacts. Human hearing is limited (20 Hz to 18 kHz). If the vibrational frequency is too fast, too high a frequency (>18 kHz), we can't hear it. Thus, ultrasound is a sound wave where vibrations are too fast for us to hear. The broad classification of ultrasound as sound above 18 kHz and up to 10 MHz can be subdivided into three distinct regions; low frequency or power (18-100 kHz), medium frequency or therapeutic ultrasound (0.7-3 MHz) and high frequency or diagnostic ultrasound (3-10 MHz) (58, 73).

The application of ultrasound waves in chemistry, sonochemistry, is well documented (122) and from many chemical reaction studies it has been found that it has an influence on reaction rate kinetics and the sonochemical effects results in reduction in reaction time, higher yield and saving in energy (116,117). Sonochemistry normally uses frequencies between 20 and 40 kHz. The origin of sonochemical effects in liquids due to ultrasound principally derives from acoustic cavitation which serves as an effective means of concentrating the diffuse energy of sound (125). Since acoustic cavitation in liquids can also be generated well above 40 kHz, recent researches into sonochemistry use a much broader range.

Ultrasound waves which alternately compress and stretch the molecular spacing of the medium through which it passes. Thus, the average distance between the molecules in a liquid will vary as the molecules oscillate about their mean position. If a large negative pressure, i.e. sufficiently below ambient is applied to the liquid so that the distance between the molecules exceeds the critical molecular distance necessary to hold the liquid intact, the liquid will break down and voids will be created, i.e. cavitation bubbles will form. When produced in a sound field at sufficiently high power, the formation of cavitation bubbles will be initiated during the rarefaction cycle. Those bubbles will grow over a few cycles taking in some vapour or gas from the medium to an equilibrium size which matches the frequency of bubble resonance to that of the sound frequency applied. The acoustic field experienced by an individual bubble is not stable because of the interference of other bubbles forming and resonating around it. As a result some bubbles suffer sudden expansion to an unstable size and collapse violently. It is the fate of these bubbles when they collapse results in the generation of intense local heating, high pressures, and very short lifetimes (73). These hotspots have temperatures of roughly 5000°C, pressures of about 1000 atm, and heating and cooling rates greater than 10^9 K/sec (5,123). Thus, cavitation can produce extraordinary physical and chemical conditions in an otherwise cold liquid (125).

There are two basic types of cavitation: stable and transient (inertial) (29). In transient or inertial cavitation, bubbles grow above their resonant size and then collapse violently. A series of effects can occur as a result of this type of cavitation: shock waves may be propagated; acoustic energy is often converted to heat yielding high microscopic

temperatures (3,36); high fluid velocities can be generated; and free radicals might be formed (31). Stable or non-inertial cavitation, a less violent event, refers to bubbles that pulsate about some equilibrium radius and often persist for many acoustic cycles (65). As a result of these oscillations, streaming of surrounding liquid occurs and mechanical stresses create mixing of the medium.

The use of ultrasound in medicine has also gained popularity due to its potential applications both in therapy as well as in medical diagnosis in recent years. Medical ultrasound generally uses frequencies between 1 and 10 million hertz (1-10 MHz). Potentially, both stable and transient cavitation may induce membrane permeabilization. Liu *et al.* (67) reported that disruption of red blood cell membranes by ultrasound correlates better with the occurrence of stable cavitation. On the other hand, other investigators (33,79) postulated that ultrasound-induced cell damage results from inertial (transient) cavitation.

Tezel *et al.* (135) have reported detailed investigations of the occurrence of cavitation during low-frequency sonophoresis. Cavitation was monitored by recording pressure amplitudes of subharmonic emission and broadband noise at four different ultrasound frequencies in the range of 20-100 kHz and at various intensities in the range of 0-2.6 W/cm^2. Enhancement of skin conductivity, in the presence of sodium lauryl sulfate (SLS), was also measured under the same ultrasound conditions. Enhancement of skin conductivity correlated well with the amplitude of broadband noise, which suggests the role of transient cavitation in low-frequency sonophoresis. No correlation was found between the subharmonic pressure amplitude and conductivity enhancement. Results of Sundaram *et al.* (121) further support the role of transient cavitation in ultrasound mediated membrane permeabilization. They have developed a mathematical model to relate the effect of ultrasound with the number of transient cavitation events. The model also allowed assessment of the role of various stages of transient cavitation, including bubble expansion, collapse, and subsequent shock wave formation, in reversible as well as irreversible membrane permeabilization. Bubble expansion and collapse, as well as shock wave, were found to contribute toward membrane permeabilization. However, a systematic dependence of membrane permeabilization on ultrasound or cavitation parameters is not yet known (121).

Generation of ultrasound

An ultrasound generator generates electrical oscillations of ultrasonic frequency (e.g. above 20 kHz). Transducer, an electro-mechanical component is a device that converts one form of energy into another. The major component of a transducer is a crystal of piezo-electric material. The transducer sends out sound waves which are partially reflected by the medium in which they are propagating, the other part penetrates and propagates into the medium. During its propagation, a wave is partially scattered and absorbed by the medium, resulting in attenuation of the emitted wave; the lost energy is converted into heat.

Sonophoresis method

The basic principle of application of ultrasound for transdermal drug delivery is to use an ultrasound source at the skin with the drug interspersed (in solution) between the transducer and the skin surface. A voltage is then applied to the ultrasound transducer at the resonance frequency of the piezo-electric crystal. This results in various effects as discussed in the following section and thereby facilitates the delivery of the drug through the skin barrier. To ensure the effective transmission of ultrasound, a coupling medium (generally a gel or water) is interposed along with the drug component between the transducer and the skin. The viscosity of the coupling agent and the quantity of the gas dissolved in the medium may significantly affect the transdermal transport (81). A decrease in sonophoretic transport of insulin and vasopressin was reported *in vitro* when molecules were administered in a gel as compared to administering them as saline solution (145). The reason for this reduction has been explained by boundary layers that form within the gel owing to the relatively rapid rate of molecular transport across the (ultrasonically) permeated stratum corneum as well as poor diffusive mass transfer between the skin and gel. The following Fig. 3 further provides a clear evidence where exposing hairless mouse to ultrasound in presence of evans blue gives intense staining of the skin, when the administration is in the form of liquid. Alternatively, administering in the form of gel gives a less intense staining of the skin. Whereas, administration without the application of ultrasound leads to very less staining of the skin (Tachibana, unpublished work) (Fig. 3).

Similar findings were reported with lidocaine *in vivo* in hairless mice (128). Tachibana and Tachibana (126) have used ultrasonic vibration to deliver insulin through the skin of hairless mice fasted overnight and partially immersed in an aqueous solution of insulin (20 units/ml). The skin surface was exposed to ultrasonic vibration in two ultrasonic energy ranges (3000-5000 Pa and 5000-8000 Pa) at 48 kHz for 5 min. Blood glucose concentration was measured before and after exposure to insulin and ultrasonic vibration. In the group subjected to the lower energy vibrations, blood glucose fell to reach 34 ± 11.9% of control values in 120 min, while when the animals were exposed to higher energy vibrations, the fall in blood glucose was 22.4 ± 3.9% of control values at 120 min. The values remained low for the length of the experiment (240 min). Those exposed to insulin alone or ultrasonic vibration alone revealed no significant change in blood glucose concentration. They have postulated that ultrasonic vibration may alter skin permeability resulting in the absorption of insulin. That the

blood glucose decrease was greater at the higher of the two energy ranges, suggests this factor could control insulin delivery. Mitragotri *et al.* (83) have found that low-frequency ultrasound did not induce a long-term loss of the barrier properties of the skin (*in vitro*) or damage to living skin of hairless rats. At a mechanistic level, they have hypothesized that application of low-frequency ultrasound enhances transdermal transport through aqueous channels in the SC generated by cavitation-induced bilayer disordering. Support for this hypothesis has also been provided using experimental and theoretical analyses of low-frequency sonophoresis.

Over the last several years, research on low-frequency sonophoresis generally classified into two categories; simultaneous sonophoresis and pretreatment sonophoresis. Simultaneous sonophoresis; this approach corresponds to a simultaneous application of drug and ultrasound to the skin. This was the first mode in which low-frequency sonophoresis was shown to be effective. This method enhances transdermal transport in two ways: a) enhanced diffusion through structural alterations of the skin, and b) convection induced by ultrasound. Transdermal transport enhancement induced by this type of sonophoresis decreases after ultrasound is turned off (89). Although this method can be used to achieve a temporal control over skin permeability, it requires that the patients use a wearable ultrasound device for drug delivery. In the pretreatment method, a short application of ultrasound is used to permeabilize skin prior to drug delivery. The skin remains in a state of high permeability for several hours. Drugs can be delivered through permeabilized skin during this period. In this approach, the patient does not need to wear the ultrasound device (91). Katz *et al.* (51) used this pretreatment method with low-frequency ultrasound to shorten the lag-time for analgesic agent to be effective.

Selection of ultrasonic parameters

The phenomenon of bubble growth and collapse and hence the lifespan of these bubbles are dependent on various ultrasonic parameters, for example, amplitude of the acoustic pressure, environmental pressure, frequency, characteristics of the liquid (such as viscosity, vapour pressure, etc.) and existence of dissolved gas in the liquid. Thus, ultrasound assisted transdermal drug delivery is affected by different parameters of ultrasound out of which some of the important parameters that affects the phenomenon to a great extent are discussed below.

– *Frequency*: The frequency F of an emitted ultrasonic wave depends on the thickness of the piezo-electric crystal. Attenuation of an acoustic wave is inversely proportional to its frequency. Thus, with an increase in frequency, the ultrasound penetrates to a greater depth into and under the skin. Since, the outer layer of epidermis, the stratum corneum, is the main barrier to percutaneous penetration of drugs, it initially seemed logical to concentrate the ultrasonic energy on this skin layer using very high frequency (10-20 MHz) in order to achieve a higher transdermal enhancement (10,11). In addition, these high frequencies were tried in early trials in order to avoid potential safety issues (58).

Bommannan *et al.* (11) have made theoretical investigations as well as experimental verifications about ultrasound propagation in tissue and predicted that higher

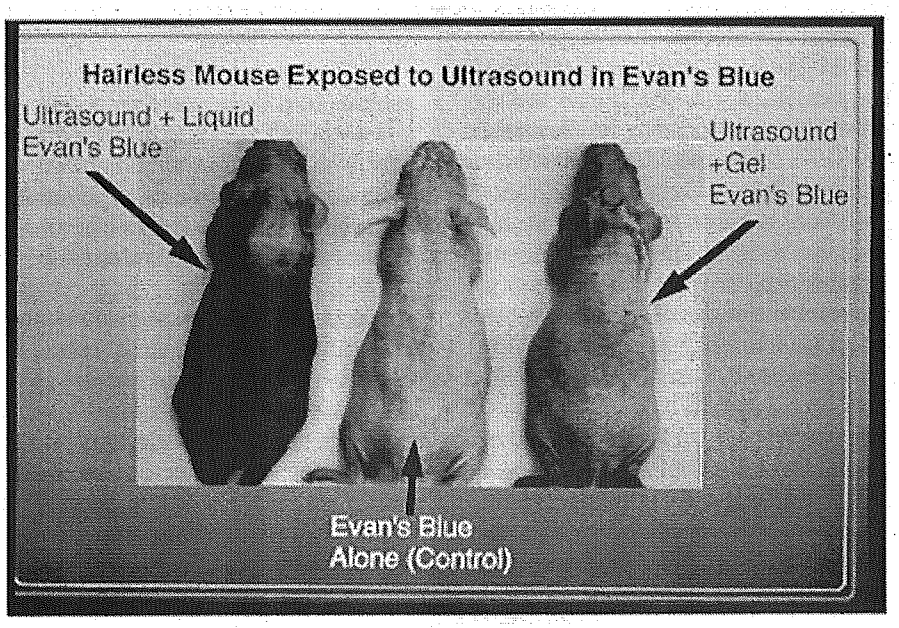

Fig. 3 Effect of ultrasound and the form of drug in staining the hairless mouse skin

frequency ultrasound (>1 MHz) increases the concentration of energy deposition in the stratum corneum. In their experiments, salicylic acid was subjected to passive transdermal delivery under the influence of ultrasound at 2, 10 and 16 MHz frequencies. Sonophoresis for 20 min at 2 MHz caused no significant increase in salicylic acid delivery over passive diffusion. Treatment with ultrasound at 10 and 16 MHz, on the other hand, significantly elevated salicylic acid transport, by 4-fold and 2.5-fold, respectively. A shorter period of 5 min of sonophoresis again resulted in enhanced transdermal transport at higher frequencies. They found that the enhancing effect of sonophoresis is due to a direct effect of ultrasound on the stratum corneum.

Mitragotri *et al.* (82) reported that the sonophoretic enhancement in the therapeutic frequency range varies inversely with ultrasound frequency. They found that 1-MHz ultrasound enhances transdermal transport of estradiol across human cadaver skin *in vitro* by 13-fold, but that 3-MHz ultrasound at the same intensity induces an enhancement of only 1.5-fold. They further hypothesized that the observed inverse dependence of sonophoretic enhancement on ultrasound frequency occurs because cavitational effects, which are primarily responsible for sonophoresis, vary inversely with ultrasound frequency (82).

The effects of therapeutic ultrasound (1 MHz, 1.4 W/cm^2, continuous) with different types of chemical enhancers on the transdermal transport of corticosterone and four other model drugs dexamethasone, estradiol, lidocaine and testosterone was investigated by Johnson *et al.* (50). Typical enhancements induced by therapeutic ultrasound are ~10-fold (20). Thus such enhancement might be sufficient for local delivery of drugs like corticosterone, but not for systemic delivery of drugs (10, 11, 58).

As cavitation could be more easily and effectively generated at low frequencies, it was then found that any frequency lower than that corresponding to therapeutic ultrasound frequency (0.7-3 MHz) should be more effective in enhancing transdermal drug delivery. This is a direct consequence of reduced acoustic cavitation at high ultrasound frequencies, due to the fact that the time between the positive and negative acoustic pressures becomes too short. In addition, the number and size of cavitation bubbles generated decreases as the frequency increases (132,134). Thus, the use of low frequency ultrasound rather than therapeutic ultrasound was shown to be more effective in enhancing membrane permeability and hence transdermal transport and has been more successful in recent years (81,128). For example, Tachibana and Tachibana (126) and Tachibana (127) have reported that the use of low frequency ultrasound (48 KHz) enhanced transdermal transport of insulin across diabetic rat skin. Merino *et al.* (78) have investigated the ultrasound effects of low (20 KHz) and high (10 MHz) frequency for the transdermal transport of mannitol. They observed that only low frequency ultrasound resulted in significantly increased permeation as compared to high frequency. Tachibana and Tachibana have used low frequency ultrasound at 48 kHz for delivering lidocaine to hairless mice (128). From their studies it was observed that ultrasound with 2% lidocaine rapidly induces an anesthetic effect. Application of ultrasound at 20 kHz induced transdermal transport enhancements of up to 1000 times higher than those induced by therapeutic ultrasound for low molecular weight drugs and high molecular weight proteins (81,83). Following table (from ref. 83) provides different types of drugs and their corresponding penetration enhancements using low frequency ultrasound (20 kHz). Here, penetration enhancement has been defined as the ratio of skin permeability when ultrasound was applied (P_{US}) and the control skin permeability (P_C) (Table 1).

A detailed investigation of the dependence of permeability enhancement on frequency in the low frequency regime (20-100 kHz) has been reported by Tezel *et al.* (134). At a given intensity, the enhancement decreased with increasing ultrasound frequency. For example, the enhancement decreased dramatically from about 45-fold at a frequency of 19.6 kHz to negligible at a frequency of 93.4 kHz with a constant ultrasound intensity of 0.84 W/cm^2. Such a strong dependence of permeability enhancement on ultrasound frequency is an indicator of the role of cavitation in low frequency sonophoresis (91).

Table 1 Drugs and their corresponding penetration enhancements using low frequency ultrasound (20 kHz)

Compound	Hydrophilicity	MW (Da)	Penetration Enhancement (P_{US}/P_C)
Aldosterone	slightly hydrophilic	360	1400
Butanol	slightly hydrophilic	74	29
Corticosterone	slightly lipophilic	346	80
Estradiol	very lipophilic	272	3
Salicylic acid	Hydrophilic	138	400
Sucrose	Hydrophilic	342	5000

Although lower frequencies induce higher enhancements, the transport at low-frequencies was found to be localized to certain areas termed as localized transport pathways (134). With an increase in ultrasound frequency, the transport was found to be more homogeneous. The optimum appears to be around 60 kHz where significant transport enhancements can be obtained with reasonable energy doses while simultaneously achieving reasonable homogeneity of the transport pathways (91).

The *in vivo* and the *in vitro* correlation of the effects of low frequency ultrasound on the percutaneous penetration of mannitol, a hydrophilic permeant, was investigated using three *in vitro* skin models and *in vivo* pig as the animal

model, in order to predict the effects of low frequency ultrasound *in vivo* on the transdermal delivery of hydrophilic permeants. The results of the study suggest that low frequency ultrasound represents a good method of enhancing the systemic absorption of hydrophilic permeants, while it does not significantly alter the vehicle-to-skin partition coefficient for the same class of permeants (130).

A more recent study by Tang *et al.* (131) identifies the critical type(s) and site(s) of cavitation that are responsible for skin permeabilization during low frequency sonophoresis using pig full-thickness skin and the effect of low frequency ultrasound (20 kHz) on the skin permeability was monitored by measuring the increase in the skin electrical conductance. An acoustic method, as well as chemical and physical dosimetry techniques, was utilized to monitor the cavitation activities. The study showed definitively that ultrasound-induced cavitation is the key mechanism via which low frequency ultrasound permeabilizes the skin. By selectively suppressing cavitation outside the skin using a high-viscosity coupling medium, they have further demonstrated that cavitation occurring outside the skin is responsible for the skin permeabilization effect, while internal cavitation (cavitation inside the skin) was not detected using the acoustic measurement method under the ultrasound conditions examined. From the acoustic measurement of the two types of cavitation activities (transient *vs.* stable), they indicated that transient cavitation plays the major role in low frequency ultrasound induced skin permeabilization. Through quantification of the transient cavitation activity at two specific locations of the low frequency ultrasound system, including comparing the dependence of these cavitation activities on ultrasound intensity with that of the skin permeabilization effect, they have demonstrated that transient cavitation occurring on, or in the vicinity of, the skin membrane is the central mechanism that is responsible for the observed enhancement of skin permeability by low frequency ultrasound (131).

Kushner *et al.* (56) recently demonstrated the existence of hypothesized localized transport regions (LTRs - localized regions of high permeability) responsible for the enhanced permeability during low frequency sonophoresis experimentally. They found an enhancement of higher than 80-fold of calcein permeability in the presence of LTRs. Also, an analysis based on porosity/tortuosity ratio suggests that trans-cellular transdermal transport pathways are present within the highly permeable and highly structurally perturbed LTRs (56).

– *Mode of application* (Pulse or continuous): Ultrasound waves can be applied continuously (continuous mode) or in a pulse (sequential, discontinuous) mode. In continuous mode, the ultrasound waves are persistent and thus the heat will be transferred to the body tissues resulting in greater heating effect (tissue heating). Whereas, the "pulsed" has the option of on/off cycles, each component of which can be varied so that the waves go in short pulses thereby altering the dose of ultrasound applied and thereby preventing the tissue heating (98). This heating effect may have a deleterious effect on sonophoresis. Tissue heating can become very painful, necessitating continuous motion of the ultrasound head, which diffuses the ultrasonic energy over a larger area. With pulsed-wave ultrasound, patients can tolerate a virtually stationary sound head, ensuring a more concentrated ultrasound dosage at the treatment site (6). Thus, the choice of pulsing mode is generally followed just to minimize the associated thermal effects. But, either form at low intensity will produce non-thermal effects. Experiments performed on hairless rats clearly demonstrate that the sonophoresis efficiency appeared to be highly dependent on the net exposure time and the ultrasound pulse "on" duration (14).

Boucaud *et al.* (12) have investigated the dependence of ultrasound-induced transdermal delivery of insulin *in vivo* to hairless rats using 20 kHz ultrasound applied over a range of pulse length. Change in blood glucose levels of the animals was monitored to assess insulin transport. The findings indicated that sonophoretic enhancement is dependent on length of ultrasound pulse that is consistent with a cavitation-based mechanism.

The effect of pulsed output ultrasound (1 MHz) with on/off ratios of 1:2, 1:4 and 1:9 on transdermal absorption of indomethacin from an ointment was studied in rats by Asano *et al.* (4). 1:2 pulsed output ultrasound appeared to be the most effective in improving the transdermal absorption. They have also found that with pulsed output it was possible to use higher intensities of ultrasound without increasing skin temperature or damaging skin.

Cagnie *et al.* (20) have examined the influence of ultrasound on the transdermal delivery of ketoprofen in humans and compared the concentrations found after continuous and pulsed application. For this purpose, one group of persons was administered ketoprofen gel using continuous ultrasound (1 MHz, 1.5 W/cm^2, for 5 min). Second group received the same treatment but with pulsed ultrasound (100 Hz, 20% duty cycle). Biopsies of adipose tissue and synovial tissue were taken during surgery to evaluate the local penetration of the drug. Blood samples also were collected to determine whether ketoprofen entered the systemic circulation. The concentration of ketoprofen in fat tissue and synovial tissue was consistently higher in the group of people administered with pulse ultrasound as compared to the people administered with continuous ultrasound.

Benson *et al.* (8) found that pulsed-output ultrasound provided the most effective conditions in the technique of sonophoresis of lignocaine and prilocaine from EMLA (eutectic mixture of local anaesthetics) cream. Nevertheless, conflicting results have also been reported concerning its occurrence during pulsed ultrasound versus continuous